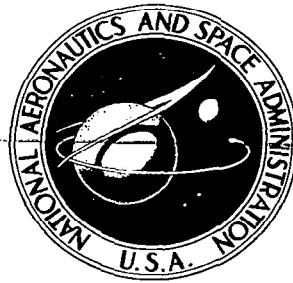


**NASA CONTRACTOR
REPORT**



NASA-CR-

0099414



NASA CR-606

LOAN COPY: RETURN TO
AFWL (WLIL-2)
KIRTLAND AFB, N MEX

A THEORETICAL ANALYSIS OF THE VISUAL ACCOMMODATION SYSTEM IN HUMANS

by Hewitt D. Crane

Prepared by
STANFORD RESEARCH INSTITUTE
Menlo Park, Calif.
for Ames Research Center

NATIONAL AERONAUTICS AND SPACE ADMINISTRATION • WASHINGTON, D. C. • SEPTEMBER 1966



A THEORETICAL ANALYSIS OF THE VISUAL
ACCOMMODATION SYSTEM IN HUMANS

By Hewitt D. Crane

Distribution of this report is provided in the interest of
information exchange. Responsibility for the contents
resides in the author or organization that prepared it.

Prepared under Contract No. NAS 2-2760 by
STANFORD RESEARCH INSTITUTE
Menlo Park, Calif.

for Ames Research Center

NATIONAL AERONAUTICS AND SPACE ADMINISTRATION

For sale by the Clearinghouse for Federal Scientific and Technical Information
Springfield, Virginia 22151 - Price \$2.50

FOREWORD

This report was prepared by Stanford Research Institute under Contract NAS 2-2760, with Dr. Hewitt D. Crane as Project Leader. The project was monitored at Ames Research Center, National Aeronautics and Space Administration, Moffett Field, California, by Mr. Richard Weick.

ABSTRACT

This study has attempted to model the human visual-accommodation system, starting directly with the retinal image. The models that are developed are reasonably consistent with existing data and offer a certain degree of understanding of certain features of the data. The modeling is in three stages. Starting at the retina we ask: (1) What portion of the retinal picture is involved in accommodation control, (2) How that portion of the picture is processed to derive a measure of defocus, and (3) How that signal in turn is used to control the ciliary muscles.

We tentatively conclude that the relevant portion of the retina is a central region of the fovea, having a diameter of some 30 minutes of arc, or 6 mils—the diameter of a coarse human hair. As for processing of the retinal image, it is shown how neural circuits based on lateral inhibition can yield a measure of defocus that is consistent with experimental data over several orders of magnitude of object size and illumination. It is also shown how interaction between three such overlapping receptor regions could account for certain chromatic effects in accommodation control. As for the control system, we tentatively propose an intermittent control model in which accommodation correction cycles may be initiated by relatively abrupt changes in the retinal pattern, caused for example by involuntary eye-movement saccads or certain target movements. The case is argued for a control cycle involving a sampling of the accommodation error followed by a ballistic corrective movement. In terms of this control model the elusive lens “vibrations” appear to be no more than normal accommodation correction cycles, what we have termed “accommodation saccads.” Apart from its role in accommodation control it is also noted how these lens vibrations could possibly increase the depth of field for strong accommodation. The models predict significant interaction between accommodation control and eye-movements. A number of experiments are proposed which would help elucidate the nature of this interaction.

CONTENTS

FOREWORD	iii
ABSTRACT	v
LIST OF ILLUSTRATIONS	ix
ACKNOWLEDGMENTS	xiii
I INTRODUCTION	1
A. General	1
B. Accommodation	1
C. Role of the Fovea	2
D. Voluntary Accommodation Control	3
E. Discussion and Outline of the Report	3
II ROLE OF VIBRATION IN OPTICAL RANGE FINDING AND AIMING	7
A. Nonlinear Photocell	7
B. Role of Vibration	9
C. Point Object	10
D. Line and Disk Objects	10
E. Nonideal Pictures	12
F. Comment on Aiming	12
III VIBRATION IN THE HUMAN ACCOMMODATION SYSTEM	17
A. Introduction	17
B. Accommodation Vibration Data	17
C. Reaction Time	19
D. Conscious Perception of Blur	20
E. Discussion of Vibration Role	22
IV IMAGE PROCESSING BASED ON NONLINEAR RECEPTORS	25
A. Receptor Cell Nonlinearity	25
B. Small Object: Point Source	25
Erroneous Response	26
Off-Center Image	26
C. Discussion	27
V IMAGE PROCESSING BASED ON TOTAL SPATIAL DERIVATIVE	29
A. Discussion	29
B. Light Intensity Threshold as a Function of Pattern Size	30
C. Light Intensity Threshold as a Function of Defocus Magnitude	32
D. Limitations of the Model	33

CONTENTS (concluded)

VI	SPATIAL DERIVATIVES BY NEURAL CIRCUITRY	35
	A. Lateral Inhibition	35
	B. Neural Unit	36
	C. Peak Detection	39
	D. Dynamics of Neural-Unit Processing	40
VII	IMAGE PROCESSING BASED ON PEAK VALUE OF DERIVATIVE	43
	A. Peak Detection over the Field	43
	B. $G(z)$ Curves	44
	C. Lateral Movement of the Image	44
	Experiment: Edge Polarity	45
	Note on Stabilized Images	46
	D. Error in Initial Direction of Response	46
	Experiment: Dependence on Initial Eye Position	47
	E. Ring Model	47
VIII	CHROMATIC ABERRATION IN ACCOMMODATION CONTROL	49
	A. Multiple Receptor Fields	49
	B. Control Algorithm; Range of Control	51
	Red-Blue Control	51
	Red-Green-Blue Control	52
	Experiment: Shifted Color Patterns	52
	C. Monochromatic Light	53
	Experiments: Monochromatic Illumination	53
IX	PROGRAMMING THE RESPONSE	55
	A. Recapitulation	55
	B. Dynamic Response	55
	C. Fixation Saccads	55
	D. Intermittent Control Model	56
	Classifying Pattern Changes	57
	Experiment: Reaction Time for Different Target Movements	58
	Experiment: Timing Target Movement to Saccadic Movement	58
	Experiment: Laterally Moving Objects	58
	E. Hypothesis: Lens Vibrations as "Accommodation Saccads"	59
	Experiment: Effect of Edge Orientation	60
X	SUMMARY	61
	REFERENCES AND BIBLIOGRAPHY	63
	APPENDIX I: DETERMINING BLURRED EDGE PROFILES	69
	APPENDIX II: LENS VIBRATION AS A MECHANISM FOR INCREASED DEPTH OF FIELD	73

ILLUSTRATIONS

Fig.	II-1 Photocell Configuration	7
Fig.	II-2 Optical Arrangement for Calculating $G(z)$	8
Fig.	II-3 $G(z)$ and $G(t)$ Curves	9
Fig.	II-4 Coordinate System and Geometrical Relations for a Circular Disk Object	11
Fig.	II-5 Photocell Signals for Different Distances between Optical System and an Approaching Man	13
Fig.	II-6 Photocell Signals for Different Angular Displacements of a Point Object	14
Fig.	III-1 Frequency Spectra of Small-Large Pupil Experiment	18
Fig.	III-2 Mean Value of Accommodation Fluctuations as a Function of the Average Value of Accommodation	18
Fig.	III-3 Records of Accommodation Responses	20
Fig.	III-4 Threshold Amplitude of Sinusoidal Distance Vibration to Detect Blur as a Function of Different Average Values of Defocus	21
Fig.	III-5 Line-Spread Function in Living Human Eye from Measurements of Reflected Aerial Image of Line Filament	21
Fig.	III-6 Geometry of Focus for a Point Object, Including Approximation to Account for Spread Function	22
Fig.	IV-1 $G(z)$ Curves for Different Locations of a Point Source on a Finite Receptor Field	26
Fig.	V-1 Relationship between Test Object Size and Threshold Luminance for Accommodation Reflex.	30
Fig.	V-2 Blur Image for a 5' Disk, 3 Diopters out of Focus, Assuming an 8 mm Pupil	31
Fig.	V-3 Effect of Scaling Object Size by a Constant k	31
Fig.	V-4 Effect of Power of Negative Lens Used to Induce Accommodation on Threshold Luminance for the Reflex for a 1° Test Object	32
Fig.	V-5 Optical Configuration for a 60' Target, 8 mm Lens, and Average Total Refraction of about 60 Diopters	33
Fig.	VI-1 One-Dimensional Lateral Inhibition Network	35
Fig.	VI-2 Form of Neural Unit	36
Fig.	VI-3 Neural Unit Processing of Black-White Transition Edge	37
Fig.	VI-4 Computer Plots of Output for Defocused Edge Patterns, Based on Neural Unit Processing	38

ILLUSTRATIONS (concluded)

Fig. VI-5	Plot of Peak Value of Output as a Function of Defocused Edge Width, from Computer Simulation of Neural Unit	38
Fig. VI-6	Computer Plots of Output for Various Bar Patterns, Based on Neural Unit Processing	39
Fig. VI-7	Transiently Enhanced Edge Sharpening with an Abrupt Edge Change	40
Fig. VI-8	Width of Gradient (α) Required for Bands to be Visible in Mach Pattern Oscillated at Various Frequencies (cps) for 4 Different Amplitudes of Motion (ϕ)	41
Fig. VII-1	Optical Geometry for a Disk Image	43
Fig. VII-2	Lateral Shift of Peak Position with Focus Change	45
Fig. VII-3	Lateral Shift of Image Position Caused by Axial Shift in Equivalent Lens Position with Change in Accommodation	45
Fig. VII-4	Potential Ambiguity Caused by an Abrupt Focus Change	46
Fig. VII-5	Ten Responses with Five Initial Errors of Response	47
Fig. VII-6	Effect of Lateral Movement on Intercept of Edge Across Receptor Field	48
Fig. VIII-1	Difference in Focus as a Function of Wavelength of Illumination	49
Fig. VIII-2	Action Spectra of the Color Pigments	50
Fig. VIII-3	Separation of Color Fields Due to Chromatic Aberration	51
Fig. IX-1	Relationship between Change in Visual Angle and Change in Target Position	58
Fig. IX-2	Compound Response with Overshoot Due to Eye Movement Occuring Soon after Target Movement	60
Fig. AI-1	Geometry of an In-Focus Disk Image and of the Blur Disk of an Out-of-Focus Point on the Edge	69
Fig. AI-2	Geometry Used for Claculating Edge Profile of Blurred Disk Image	70
Fig. AII-1	Geometry of an Edge Image Focused within a Stack of Elongated Receptors	73
Fig. AII-2	Edge Profile Resulting from Arrangement in Fig. AII-1	75
Fig. AII-3	Edge Profiles for Different Focus Positions within the Receptor Stack	75

ACKNOWLEDGMENTS

The author would like to acknowledge the vigorous assistance of Jim Townsend in tracking down and trying to understand the widespread literature in human lens accommodation; Jim Bliss, with whom this study was initially conceived, and who offered many interesting suggestions; and Tom Cornsweet, whose enthusiasm for the models significantly bolstered the study, and who contributed important suggestions for conducting experiments suggested by the models.

I INTRODUCTION

A. General

There are three major muscle systems that control the human visual system: the extra-ocular muscles for horizontal, vertical, and torsional eye position; the ciliary muscles that control the lens; and the iris muscles that control the pupil. Not only is the control of each system complex within itself, but the systems are complexly interrelated, so that a change in accommodation, for example, will be accompanied by a change in horizontal vergence of the eyes, and also a change in pupil size.

Although a considerable amount of experimental information has been gathered regarding each of these systems, there is still scant understanding of how control is actually achieved. There are clearly voluntary and involuntary aspects of each system. One can voluntarily change the direction of gaze, and some individuals can voluntarily change their states of vergence and accommodation. It is clear then that "higher brain centers" are involved in these control systems. Learning is also an important factor. There are even "emotional" factors in the control—pupil size has been suggested as a fairly sensitive indicator of emotional content of the retinal picture (Hess, 1965), and Westheimer (1957, p. 718) noted that anger could cause an increase in accommodation of greater than a diopter for several minutes.

When we ask what controls each of these major systems, we run onto unsure ground because the aspects of the retinal picture that are involved are not fully known. We do not yet know the nature of the neural circuitry. We have then a highly dimensioned problem with scanty knowledge of the operation of each parameter, in fact incomplete knowledge even of the complete "list" of parameters. It is little wonder then that there is controversy on many theoretical as well as experimental results. Also, the difficulty of the experimental situation generally precludes the use of large numbers of subjects. This is important because of the significant differences from subject to subject, not only quantitatively in their degree of control, but also qualitatively in their manner of control.

B. Accommodation

Our primary concern in this report is with the accommodation system. If we alter the distance of an object from the head, the differential lateral displacement of the images in each eye could not only signal the necessary vergence correction, but also could signal an appropriate change in refractive accommodation. Thus, with binocular vision there is really no logical need for monitoring focus per se. To do without monitoring, however, one would have to be born with a built-in conversion table relating accommodation and convergence. In view of the wide variation from subject to subject in eye parameters and performance, the existence of a completely functional built-in table at birth is unlikely. Much more appealing is the notion of an independent focus system, with any built-in vergence-accommodation table filled in, or at least modified, as a result of learning.

Another argument for control based on learning is the wide variation of accommodation performance with age. A newborn infant, for example, can focus only at a single target distance of about 19 cm, but by the fourth postnatal month has reached almost the full accommodation range of an adult (Haynes, White, & Held, 1965, p. 528). But even the full accommodation range of an adult decreases monotonically with age (Davson, 1962, Vol. 3, p. 207). This decrease in accommodation range as a function of chronological age is known as presbyopia.

The optimum focus condition for each eye is not only a function of horizontal vergence, but also of version—i.e., the angular displacement of the line of regard. For fixation to the side of the head there can be a significant difference in required refraction for each of the two eyes. It is not clear from the literature whether there is actually a difference in the accommodation of the two eyes under these conditions, although Abraham (1961, p. 197) implies that this may actually be the case. If this were the case, then an expanded interrelation table of vergence, version, and accommodation would have to be prewired; or again, with a separate focus system, filled-in by repeated experience.

There is a question then as to how completely the control connections from sensor apparatus to ciliary muscles are closed at birth (i.e., built-in) and how much the control connections are built-up or altered by learning.

With regard to determining the optical state of focus in a monocular system, one point seems clear: it is necessary to sample the three-dimensional space of light rays at more than just a single plane. There seem to be just two basic ways of multiply sampling the image space—one depends on moving a single receptor sheet to more than one axial position; the other depends on the use of more than one receptor sheet to simultaneously monitor different planes of the image field. The three color “layers” in the retina, in combination with chromatic aberration, can be useful in processes of the second type, and the various motions and tremors of the lens of the eye provide possibilities of the first type. With a completely static, monochromatic, unfamiliar image on a planar retina, no correct information could be obtained about the state of focus.

Fincham's results (1951) regarding the use of monochromatic light are interesting in this regard. He found that of 55 subjects, 40 percent had the same accommodation responses with monochromatic light as with white light, 35 percent had no response at all with monochromatic light (though conscious of blur), and 25 percent had certain errors in their response with monochromatic light.

One is led to suspect that several different methods of accommodation control are possible and that some people might use one or more of these capabilities simultaneously, while in others, some of these systems remain dormant, with the possibility of being evoked or trained when the subject is deprived of his more familiar signals. Certain forms of temporary or permanent color blindness, for example, might prevent the use of chromatic information for focus control.

C. Role of the Fovea

At any instant we can focus for only a single physical distance, so we require a mechanism to select just what in the field we wish to focus on. In view of the high-resolution fovea and the accurate voluntary eye-movement capability of the human, it seems logical to speculate on an accommodation control system that receives input only from some portion of the fovea and relies on eye movements to bring the point of interest “to the fovea”.

A number of experimental results make it probable that this is in fact the arrangement in the human focus system. Campbell (1954, 1st ref.), for example, concluded that the receptors for accommodation control are the foveal cones since the illumination threshold for accommodation change is only a quarter to half a log unit higher than the cone threshold for visibility. He also found (p. 14) that “if the subjects looked to one side of the test disk so that its image fell on the parafovea which is rich in rods, it could be seen when it was 100 times dimmer still, but no accommodation occurred to compensate for the negative lens.”

The fovea is generally taken to be several degrees in diameter. The central depression, the foveola, is typically taken as some 100' in diameter (about a degree and a half). The focus control seems to be confined to an even smaller central region of the foveola. Fincham (1951, p. 389), for example, found that if a subject consciously fixated as much as 10' of arc removed from a 3' black-dot object then his state of accommodation no longer tracked changes in distance of this object. Focus control seems to be limited to the central portion of the fovea, which has the very highest resolution. Plots of rod and cone density show that rod density starts to become significant by about 20' from the center of the fovea and that cone density has about dropped in half at this point (Davson, 1962, Vol. 2, p. 20).

All in all, it appears as a reasonable working hypothesis that focus control operates on signals derived from only a small central portion of the fovea, 30' or so in diameter. It may be of interest to note that a 30' disk on the retina has a diameter of about 150 μ , or 6 mils, the diameter of a coarse human hair. A primary concern in this study is the nature of the neural processing in this region that might be relevant to defocus estimation.

D. Voluntary Accommodation Control

Westheimer (1957, p. 718) noted that when viewing an empty field, subjects could transiently change their accommodation about half a diopter simply by thinking about "near" or "far." Some subjects can apparently relax their accommodation even while remaining fixated on an object. In some experimental situations, however (for example in monochromatic light), subjects, though conscious of blur, cannot voluntarily correct their focus. One is tempted to conclude that voluntary control is generally rather limited.

On the other hand, Campbell (1954) studying the effect of luminance change on the amplitude of accommodation change noted

"It should be stressed that in this experiment the subject was instructed to exert voluntarily enough accommodation to overcome the blurring due to a -6D lens and that the accommodation response was not necessarily involuntary as in the previous experiments."

These results would lead one to suspect that one can have considerable voluntary control over focus. Campbell states nothing, however, about whether these subjects were highly trained at the task.

It is not clear from the literature just how much voluntary control can be exercised, in particular how much this control can be developed with practice. This seems to be an interesting area of study and is mentioned here as a reminder that voluntary aspects may be important when evaluating results from experiments that may ostensibly be studies in involuntary control.

E. Discussion and Outline of the Report

This study was primarily motivated by the development of an optical range-finding system based on the use of an axial vibration between a lens and a "receptor sheet," namely a wide-area photocell on which the entire image falls. The nature of this system and its performance with real-world images are discussed in Sec. II. It was the analogy of this axial vibration to the reported low-frequency (approximately 2 cps) variation in focal length of the human lens that motivated the present study. (This low frequency lens vibration should not be confused with the much higher frequency whole-eye tremors.)

Some accommodation data and discussion of the lens vibration is given in Sec. III. The operation of the optical ranging system depends on the use of a nonlinear photocell whose output is therefore sensitive not only to the total light falling on it, but also to its distribution. In Sec. IV we speculate on whether the retina could be organized to operate in a corresponding way, i.e., as a sheet of nonlinear receptor elements whose outputs are linearly summed. It is concluded that this simple image-processing technique is not a likely candidate for the accommodation control system.

Models based on the use of spatial derivatives over the sensitive retinal area are far more appealing. In Sec. V we show how a model based on summing the absolute magnitude of spatial derivative over the field is consistent with certain experimental results, but has certain limitations for fine-focus control. In Sec. VI we consider how spatial derivatives can be obtained in neural circuits, and we conclude that there is probably a greater weighting on the peak values of derivative over the field. In Sec. VII we consider the consequences of a model based on peak detection over the field and show how it is consistent with a relatively broad spectrum of experimental results. In Sec. VII we extend the model to try to account for certain chromatic effects.

The material of Secs. V - VIII is primarily concerned with image-processing techniques for abstracting a measure of the state of focus. In Sec. IX we discuss how such an abstracted signal measure might be used for controlling the ciliary muscles. At this point it is important to note the interaction between accommodation control and eye movements.

The involuntary saccads have an average amplitude close to 10' of arc. Hence, even during fixation, the position of the image on which we are focusing performs quite a dance over the speculated 30' receptor region for accommodation control. It resembles somewhat the situation of attempting to focus a camera while standing on an abruptly jerking platform. We must therefore consider the effects that an eye movement—even a microsaccad—can cause in the output signal due to transients in the image-processing network. A number of experiments involving simultaneous monitoring of eye movements and accommodation are suggested in Sec. IX.

Although this study was initially aimed at evaluating the role of lens vibrations, it became apparent that an answer could be obtained only by attempting to develop a model for the entire control system. The data available in the literature are so scant and uncoordinated, however, that attempts at model-making raise more questions than they answer. The models attempted here have nevertheless stimulated a number of novel experimental approaches which may help provide a more detailed and coordinated understanding of accommodation control.

In any case, both the source and role of lens vibration are still not clear at the moment. In fact, in Sec. IX we have speculated on an entirely new notion regarding the "source" of the vibration; namely that it is a series of normal accommodation correction responses or "accommodation saccads," and not a vibration in the usual sense at all. In Appendix II we have even speculated on another potential function of the vibrations, namely that they increase the depth of field at the expense of a slight "softening" of focus over the increased range. This may be most important for strong accommodation (i.e. close-up focus) where the depth of field is nominally very small, but the vibrations are relatively large.

The reader should bear the following in mind when reading this material: the focus-control system evolved like any other biological system, and therefore we should not necessarily expect it to operate like a system that a human might design. Visual patterns are complex. Though we might be pleased to find that the system operates equally well with dark patterns and bright patterns, small and large patterns, point patterns and line and wide-area patterns, monochromatically

illuminated patterns and white-light patterns, small magnitudes of defocus and large ones, and so on, it may be well that the system is better suited for some combinations than others; in fact, it may operate incorrectly with some combinations.

In this connection, we might note the following observation by MacKay (1958):

“One interesting side-effect which we are studying is an apparent disturbance of the accommodation reflex by the circular, i.e. concentric ring, pattern. A hair laid obliquely across its central region may sometimes defy all efforts to bring it into sharp focus, although against a plain background at the same distance it becomes perfectly sharp.”

In the development of models discussed in this report, there is an attempt to single out combinations of conditions that may lead to differing and perhaps unique results. Often a potential control function appears to change form beyond a range of ± 1 diopter or so. This is of interest since many experiments are typically carried out with defocus stimuli in this range of magnitude. It may be that in some experiments the conditions are effectively just beyond the range where the control mode changes, and this may account somewhat for differences in reported results. For example, as noted in Sec. VII-D, Campbell and Westheimer found no errors in initial direction of focus correction, whereas Stark and Takahashi, in a nominally similar experiment, found almost 50 percent errors, i.e. a random choice in initial direction of correction. In both experiments the defocus magnitudes were typically 1 to 2 diopters.

Finally, it seems appropriate in the way of introduction to include several quotes from Walls (1963) to put the reader in the proper frame of mind with regard to evolutionary aspects of the accommodation system:

“As with peoples and their governments, vertebrate eyes get the kind of accommodation they deserve. The degree of “eye-mindedness” in the subphylum sinks from the higher fishes to the amphibians, rises sharply in the reptiles, still higher to a peak in the birds and falls off woefully again in the mammals—with some recovery in the highest forms and a very considerable one in the squirrels and simians, to be sure. The engineering efficiency of the accommodatory apparatus runs exactly parallel with this variation in the value set upon vision.” (p. 283).

“The extent of accommodation is very low indeed in mammals—often zero—except in the primates. The cat, which is the nearest competitor of the simians in this regard, has but half the accommodation of a thirty-year-old man and loses even this in old age. Human accommodation being ‘tops’ for mammals (Beer found no more than ten diopters in any ape), it is desirable to turn back to the graph (Fig. 15, p. 35) showing its extent at various ages. The senescent diminution of the power of accommodation in mammals is bound up with the accommodatory method itself. Certainly in the Ichthyopsida no such falling-off is to be expected, for the lens in these animals may become even harder with age than it is in the young, without this affecting the range of accommodation a particle.

. . . A special situation arises in small-eyed mammals. The squirrels are exceptional among the rodents, in having some accommodation, which we should expect from their diurnality and high visual acuity. The European squirrel may be emmetropic or as much as one-half diopter hypermetropic, and can accommodate from one to one and one-half diopters. As the size of the eye diminishes from that of a cat to that of a mouse, the increasing (relative) size and firmness of the lens and its (relative) recession toward the retina results not only in the reduction of accommodation from a couple of diopters to nothing, but also

in an increase of the hypermetropia from a half-diopter or so to five, seven, even ten diopters. . . . The cerebral images of mice and the like are so crude at best, that the eye is useful more for recording the intensity and direction of light, and the motion of large objects in the visual field, than for discrimination of pattern. In such animals, the 'nose knows' far more about the environment than does the eye." (p. 287).

As one reviews the evolutionary history of the accommodation system it appears that every conceivable optical configuration has been "tried" in some specie or another, starting with the pin-hole eye of the nautilus. The history makes an interesting tale indeed, and one that tends to restrain jumping to quick conclusions about the value or cleverness of any particular design, at least before seeing how it fits the larger picture. For example, it is often commented that the near-reflex of the eye (increased convergence, increased accommodation, and narrowing of the pupils for a close object) is a perfectly reasonable and useful form of response. Yet . . . "In the dog, according to Nicolas, the accommodation reflex works backwards—the pupil dilating for near, contracting for distant objects; and there is no consensual reflex. These peculiarities have yet to be explained." (Walls, p. 156).

II ROLE OF VIBRATION IN OPTICAL RANGE FINDING AND AIMING

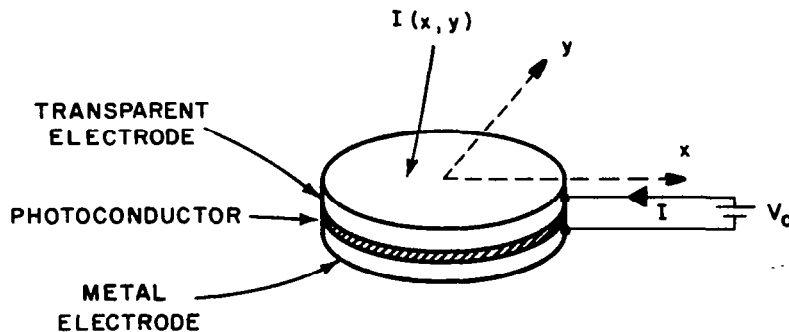
Relatively simple techniques for optical range-finding and optical aiming have been developed which involve the use of a wide-area nonlinear photodetector and certain modes of vibration in the optical system (Bliss and Crane, 1964, 1965). Development of these techniques is what led to the present study of the possible role of the microfluctuations (vibrations) of the lens in the human accommodation system. These optical techniques are briefly reviewed in this section.

A. Nonlinear Photocell

Consider a wide-area photocell, in which the photoconductive material is sandwiched between a pair of parallel electrodes, one of which is transparent, as shown in Fig. II-1. Let the illuminance of the photoconductor be denoted by $I(x,y)$, where coordinates x and y are as shown in the figure. If we assume that the conductivity at any point of the photoconductor is some function g of the illuminance at that point, i.e., $g=g[I(x,y)]$, and if we assume a thin uniform cell, then the total conductance of the cell is

$$G = \iint_A g[I(x,y)] dx dy, \quad (\text{II-1})$$

where A is the area of the photoconductive material. With constant applied voltage, current through the cell is proportional to total conductance, and we can, therefore, use cell current as a monitor of cell conductance. Our primary concern is with the manner in which this conductance, or current, varies with the axial position of the photocell behind the lens.



RA-646,541-41

FIG. II-1 PHOTOCCELL CONFIGURATION
T—Transparent Electrode
P—Photoconductor
E—Metal Electrode

Consider a simple point source of light and the resulting cone of light formed by the lens, as shown in Fig. II-2. The photocell intercepts this cone of light at a distance z from the point of focus. For a linear photoconductor material, we can write $g = kI(x,y)$, where k is a constant, so that Eq. (II-1) reduces simply to

$$G = k \iint_A I(x,y) dx dy = kL_T, \quad (\text{II-2})$$

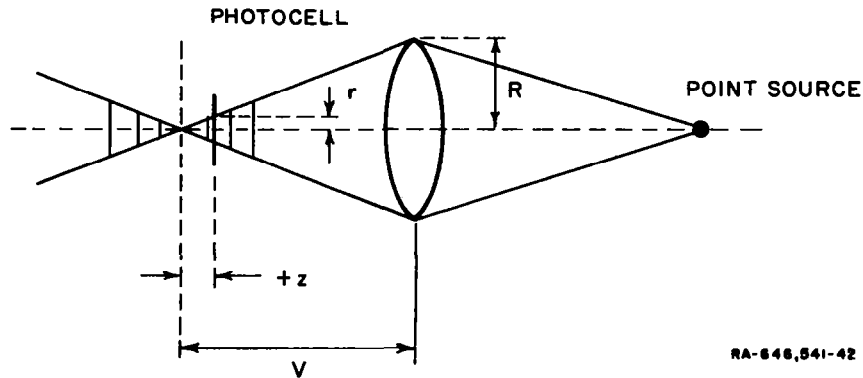


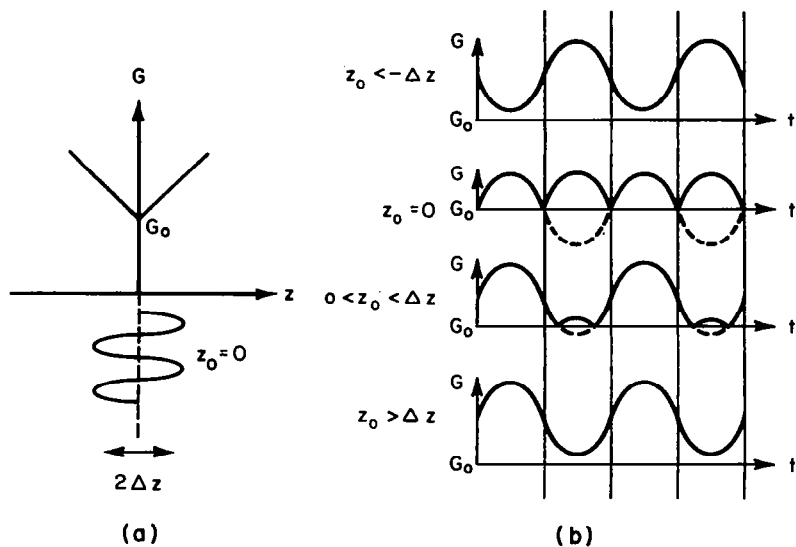
FIG. II-2 OPTICAL ARRANGEMENT FOR CALCULATING $G(z)$
 S—Point Source
 P—Photocell

where L_T represents the total light flux falling on the cell. In other words, with a linear photocell, total conductance depends only on the total flux of light and not at all on its distribution.

With a nonlinear photocell, one characterized—for example—by the relation

$$g = k[I(x,y)]^p, \quad (\text{II-3})$$

the conductance depends not only on the total light but also on its distribution. For $p < 1$, a plot of conductance vs. the position of the photocell along the z axis is an even function of z as shown in Fig. II-3(a) and has a minimum at $z = 0$. For $p > 1$ the conductance has a maximum at the origin. For $p = 1$ (i.e., a linear cell) G is, of course, independent of cell position.



RA-646541-43

FIG. II-3 $G(z)$ AND $G(t)$ CURVES
 (a) $G(z)$ Curve for $p < 1$
 (b) $G(t)$ Curves for different values of z . Peak-to-peak amplitude of photocell vibration is $2\Delta z$.

B. Role of Vibration

We see then that a nonlinear photocell is sensitive not only to total light but also to the light distribution. Suppose now that we vibrate the photocell axially about an average position $z=z_0$, and with a peak-to-peak amplitude $2\Delta z$. If $\Delta z < |z_0|$, the photocell never crosses the image plane and the resulting variation in conductance is sinusoidal (assuming for the moment a linear $G(z)$ curve). If $\Delta z > |z_0|$ the photocell crosses the image plane, the signal "folds over" as in Fig. II-3(b), and even harmonics are introduced into the signal. For $z_0=0$, the photocell vibrates exactly about the image plane and there is no fundamental at all in the output signal.

By monitoring the phase of the fundamental we can therefore sense direction of defocus, and by monitoring "fold-over", or even-harmonic content, we can obtain a measure of the magnitude of defocus. Operating in this mode, the $G(z)$ curve should be as linear as possible away from the origin, and the discontinuity at the origin should be as sharp as possible. Actually, a linear $G(z)$ curve away from the origin is possible only for a point source and an exponent $p=\frac{1}{2}$, assuming the photocell model of Eq. (II-3). Also the $G(z)$ curve is an exact even function of z only for a point source, though $G(z)$ curves for two-dimensional objects closely approximate even functions, especially if the image size is small compared with lens size.

Derivation of $G(z)$ curves (for $z > 0$) for a point, a line, and a disk are briefly outlined below. The result for the point source is used in Sec. III. These derivations are abstracted from Bliss and Crane, 1964. Experimental results for a complex pattern are indicated in Sec. E.

C. Point Object

Figure II-2 shows the coordinate system and geometrical relations for this case. The image occurs at a distance V from the lens, which has a radius R . The total light flux intercepted by the lens is L_T . Neglecting diffraction effects, a screen placed in the image plane intercepts a sharp point of light. Removed a distance z from the image plane, the screen intercepts a circle of light of uniform illuminance I_z where

$$I_z = \frac{L_T}{\pi} \left(\frac{V}{R} \right)^2 \frac{1}{z^2} = L_T / \left[\frac{\pi}{4} \left(\frac{z}{V/2R} \right)^2 \right] \quad (\text{II-4})$$

Over the circle of light, the photocell conductivity is

$$g = k I_z^p, \quad (\text{II-5})$$

or the total conductivity is simply

$$G = k \left\{ L_T / \left[\frac{\pi}{4} \left(\frac{z}{f^*} \right)^2 \right] \right\}^p \frac{\pi}{4} \left(\frac{z}{f^*} \right)^2, \quad (\text{II-6})$$

where $f^* = V/2R$ is approximately equal to the f /number of the lens (for relatively large object distances, $V \approx f$, the focal length). Thus, G is proportional to $z^{2(1-p)}$, so that for $p=0.5$ the cell conductance is linearly proportional to z .

For the case of a square lens aperture, the factor $\pi/4$ is replaced by unity and Eq. (II-6) reduces to

$$G = k [L_T / (z/f^*)^2]^p (z/f^*)^2. \quad (\text{II-7})$$

This equation is intuitively reasonable. It is basically a product of an illuminance raised to the power p , and an area (note that z/f^* is the length of a side of the intercepted square cone). For $p=1$; Eq. (II-7) reduces to kL_T ; that is, the cell is linear and G is independent of z .

It is important to note that Eq. (II-7) is unchanged if the object is moved off axis. Thus the $G(z)$ curve is independent of whether the point source is on-axis or off-axis. Extension of this result to objects other than a point source gives the important result that the photocell conductance is nominally independent of the angular position of the source objects. That is, this ranging is not limited to on-axis objects.

D. Line and Disk Objects

Let us now consider a line image of length $2D$. We can visualize a cone of light extending to each point of the image. The light in any particular cone emanates from a corresponding point of the source. Out of focus (i.e., in any plane other than the image plane), the resulting light pattern is due to the overlap of light from neighboring cones. If the light from the source is noncoherent, then the illuminance at any point is the sum of illuminance contributed from each cone.

Assuming again a square lens, we find the illuminance in an out-of-focus plane to be uniform over a width $2y$ and over a length $2x$; it falls to zero linearly over a length w on each end. (If the lens were circular, the intensity would vary across the width, the intensity taper at the ends would not be linear, and the integrals would be much more complex than with a square lens.) Following the same form of derivation as for the point source we find the total conductance to be

$$G = k \left[\frac{L_T}{(z/f^*)2D \left(1 - \frac{z}{V}\right)} \right]^2 \frac{z}{f^*} 2D \left[1 - \left(1 + \frac{p-1}{p+1} \frac{R}{D}\right) \frac{z}{V} \right] \quad (\text{II-8})$$

Now for small vibrations (i.e., $z \ll V$) where we can neglect z/V , the expression in the right-hand brackets reduces to unity and we have

$$G \approx k [L_T/2D(z/f^*)]^2 2D(z/f^*). \quad (\text{II-9})$$

This equation is reasonable, since for small z the length of the defocused line remains essentially constant and equal to $2D$, whereas the width increases as (z/f^*) , that is, linearly with z . Thus $2D(z/f^*)$ approximates the area of the intercepted light.

In practice we could not expect Eq. (II-8) to hold as z approaches zero because the illuminance becomes very large, and the photocell model of Eq. (II-3) can at best hold over a limited range of illuminance. For $z=0$, Eq. (II-8) predicts that $G=0$ or $G=\infty$ for $p < 1$ and $p > 1$, respectively.

We have been able to treat the point and straight-line image with an exact analytic treatment. For any two-dimensional object, however, exact analysis is difficult. The simplest case is a uniformly illuminated circular disk object and a circular lens, in which case the defocus patterns are independent of rotation. For example consider the arrangement of Fig. II-4(a) in which we

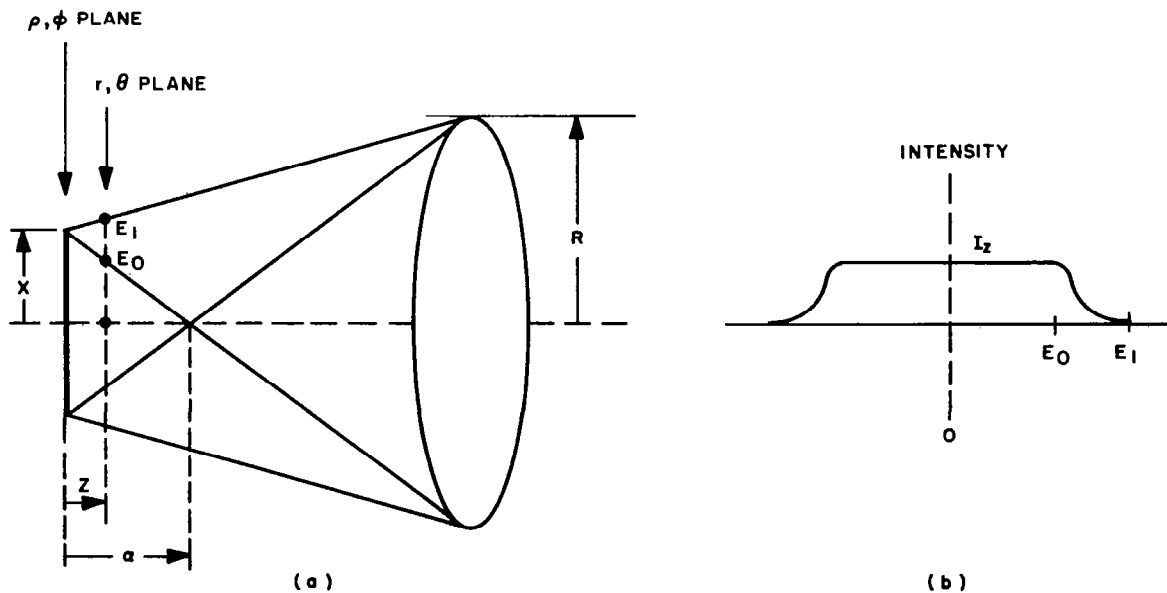


FIG. II-4 COORDINATE SYSTEM AND GEOMETRICAL RELATIONS FOR A CIRCULAR DISK OBJECT

RA-4213-17

have a circular disk image of radius X . In a plane removed a distance z from focus, the defocus image is a uniformly illuminated disk of radius E_0 surrounded by an annulus where the intensity falls off to zero at radius E_1 . The intensity profile then is as indicated in Fig. II-4(b). Note that the intensity does not fall linearly from E_0 to E_1 .

Methods for calculating the exact form of the defocused edge are discussed in Appendix I. Assuming a linear transition edge, however, in order to simplify the analysis, and assuming again that $z/V \ll 1$, we find

$$G(z) \approx k \left[L_T / \pi x^2 \left(1 - \frac{z}{V} \right)^2 \right]^p \pi x^2 \left(1 - \beta \frac{z}{V} \right)^2, \quad (\text{II-10})$$

where β is a constant depending on p , R , and X , from which we see that $G(z)$ is proportional to

$$\left[1 - (z/V) \right]^{-2p} \left[1 - \beta (z/V) \right]^2 \quad (\text{II-11})$$

In summary, we see that the $G(z)$ function for a point source is a sensitive function of defocus distance, namely z^2 . For a line source, the dependence is basically of the form $z(1 - \frac{z}{V})$, or simply z , for $z \ll V$. For a disk the dependence is even weaker, being of the form $(1 - \beta \frac{z}{V})^2$ where β depends on the relative size of the image and lens. Though we will not be concerned with this particular form of detector system in the later models that we develop, the difference in functional dependence for zero, one, and two-dimensional objects (i.e., points, lines and disks) will be similar. (For the retinal patterns that we will be interested in, any two-dimensional image will be very much smaller in extent than the lens opening, in which case the constant β in Eq. (II-11) would be equal to unity.)

E. Nonideal Pictures

For simple objects we can calculate or estimate the $G(z)$ curves, at least for a relatively simple photocell model. For a complex picture, however, the difficulty of analysis is obvious because of the complexity of the defocus patterns. In Fig. II-5 we show that the technique is nevertheless applicable to more complex pictures. Shown side by side are actual photographs of the image falling on the photocell and the corresponding electrical signals obtained directly from the photocell. The optical system consisted of a 35 mm diameter, 56 mm focal length acromatic lens vibrated axially with a peak to peak swing of a little less than 1 mm. The average position, i.e., z_0 was adjusted for focus at 6 feet. With the front "surface" of the man substantially at 6 feet, there is a strong double frequency signal. At 5 feet and at 7 feet the signal is primarily fundamental, and with opposite phase as predicted. With the man removed to infinity, just the distant out-of-focus parking lot remains and the output signal is highly sinusoidal. We see that these signals could be readily processed for detection of objects within a fixed range, or for automatic focus.

F. A Comment on Aiming

We might note that with a rotational mode of vibration, as suggested in Fig. II-6, instead of an axial vibration, the same wide-area nonlinear photocell is useful for determining angular displacement of a target, or as an input processor for an automatic aiming system. The oscilloscope pictures of Fig. II-6 are for a peak to peak rotational vibration of a few degrees. We

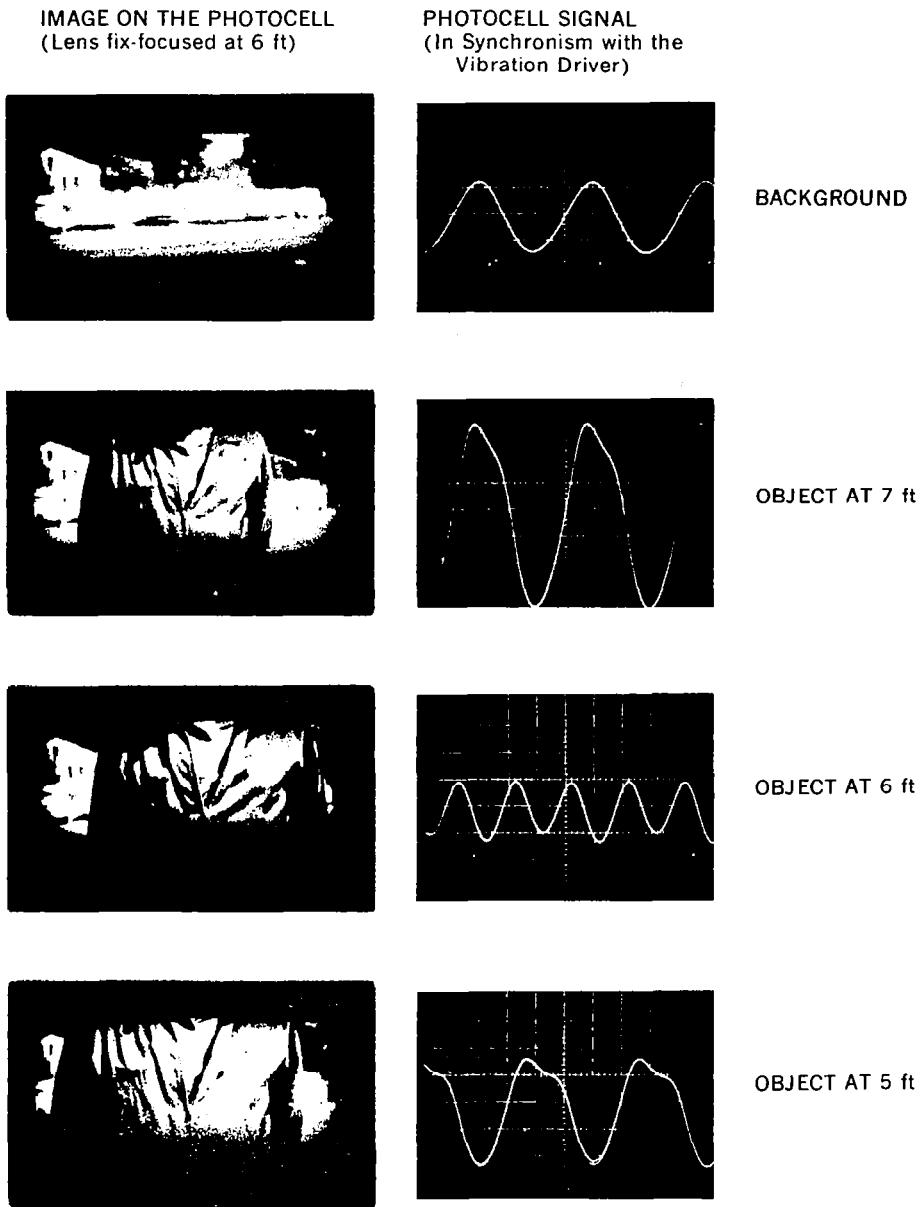


FIG. II-5 PHOTOCCELL SIGNALS FOR DIFFERENT DISTANCES BETWEEN OPTICAL SYSTEM AND AN APPROACHING MAN

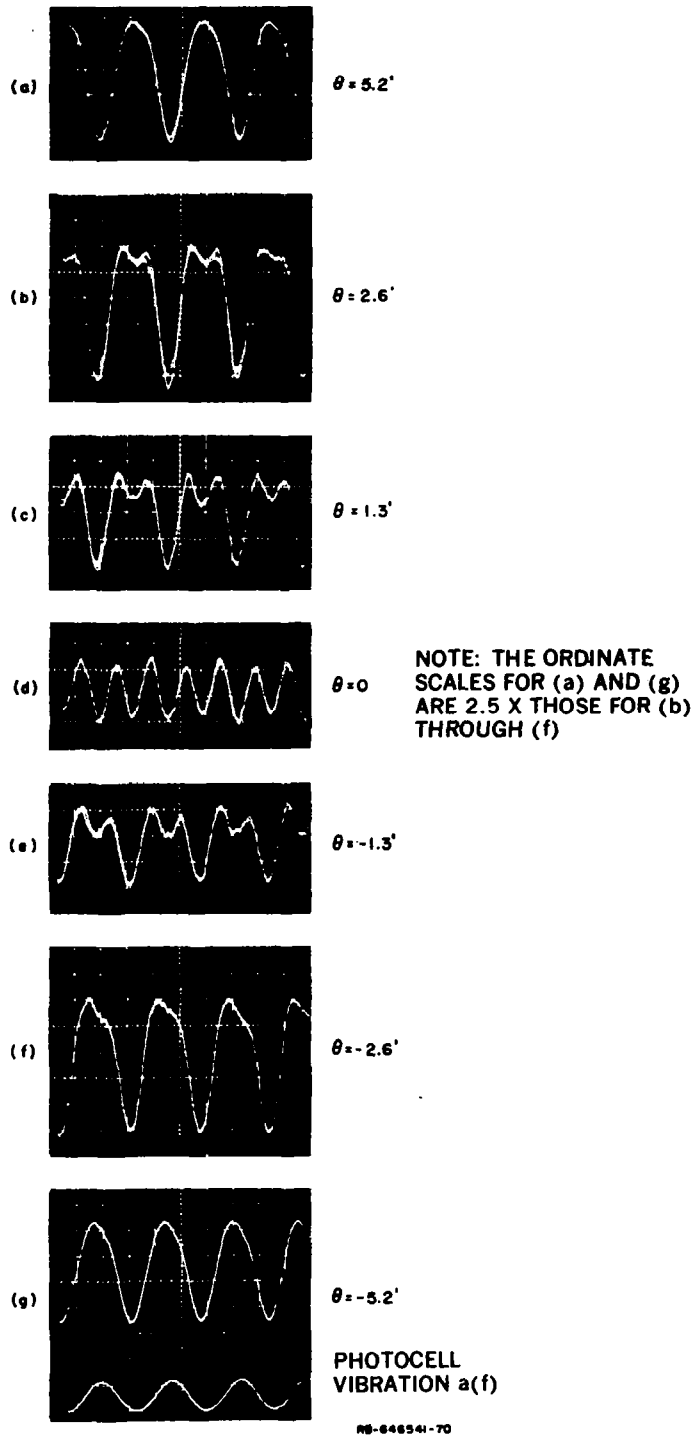


FIG. II-6 PHOTOCCELL SIGNALS FOR DIFFERENT ANGULAR DISPLACEMENTS OF A POINT OBJECT

see from the central figure that with the object (in this case a point source) directly on axis we have a strong double-frequency signal. As the object is moved progressively off-axis the signals progressively pass toward the fundamental, but of opposite phase on either side of the axis. The signal changes from a double-frequency sine wave to one having the appearance of a half-wave rectified sine wave with an angular displacement of only $1.3'$ of arc. For a further discussion of this mode of operation see Bliss and Crane, 1965.



III VIBRATION IN THE HUMAN ACCOMODATION SYSTEM

A. Introduction

To obtain a physical measure of the state of focus, we have argued the need for a multiple sampling of the three-dimensional image space. This can be effected by axially moving a single receptor sheet, or by using several axially displaced receptor sheets simultaneously. With physical optics, the former technique is readily applied, as described in the previous section. Physically arranging for a number of different sheets is more difficult. In physiological optics, systems based on both movement and multiple sheets seem to have been employed. The multiple sheets are in the form of the three color layers. Although these layers are physically within the same retinal plane, the three layers are in effect displaced from each other by almost one diopter, because of chromatic aberration. We will discuss chromatic control in Sec. VIII in terms of a model derived in Sec. VII.

For a physical movement to be useful in the measure of focus, it is necessary to have some processing system which is sensitive to the effects of the movement. In the words of Fender (1964, p. 27),

“. . . the accommodative mechanism has a steady “hunting” motion superimposed on it that continually lengthens and shortens the focal length of the lens. Depending on the location of the object being viewed, a change in one direction will improve an out-of-focus image and a change in the other direction will worsen it; this information is fed back to steer accommodation in the direction of sharpest focus.”

A primary question with regard to this hunting is just what measure of the output image is “fed back to steer the accommodation.” As to the lens vibration serving as a hunting mechanism, we must ask whether the amplitude is adequate for the purpose and whether it is present at appropriate times. The data gathered thus far about this vibration, and the manner in which it jibes with the models developed in subsequent sections, make it appear at least a reasonable candidate, though additional experimental results are required for a more definitive answer.

In the next three sections we review some of the available data on lens vibration and accommodation response in general.

B. Accommodation Vibration Data

Campbell, Robson, and Westheimer (1959) showed the accommodation fluctuation spectral plots of Fig. III-1, derived by autocorrelation processing of continuous recordings of accommodation variation. The recordings were made with a continuous-recording optometer (for details of the optometer design see Campbell and Robson, 1959). Of special interest is the peak appearing at about 2 cps. Growing numbers of investigators during the past ten years have been reporting fluctuations of lens power, particularly in this frequency range. Some data regarding this vibration are:

1. The amplitude of oscillation is typically reported at a couple to a few tenths of a diopter. It must be kept in mind, however, that all optometer results to date are for focus measurements in a single meridian only. The effective amplitude of vibration may therefore be larger than generally reported.

2. Arnulf and Dupuy (1960) report a monotonic increase in amplitude with accommodation magnitude, reaching a peak-to-peak amplitude of 0.7-2.0 diopters for one subject accommodated to an average value of 6.8 diopters, Fig. III-2, though exactly what components are included in this fluctuation measure is not clear from the article.
3. The oscillation amplitude is greatly reduced (as seen in Fig. III-1) if a small artificial pupil is inserted in the optical path, with the illumination increased to maintain constant image intensity. Thus, the fluctuations are not simply the result of closed-loop instability involving the depth-of-field dead zone. Warshawsky (1963, p. 10) reviews some of the arguments regarding stability of the accommodation (and pupillary) control system. Stark (1965), on the other hand, concludes that the vibration is a control system instability.

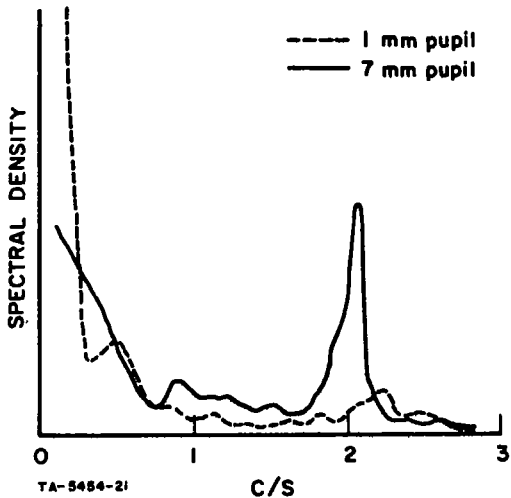


FIG. III-1 FREQUENCY SPECTRA OF SMALL-LARGE PUPIL EXPERIMENT

Source: Campbell, Robson, and Westheimer (1959)

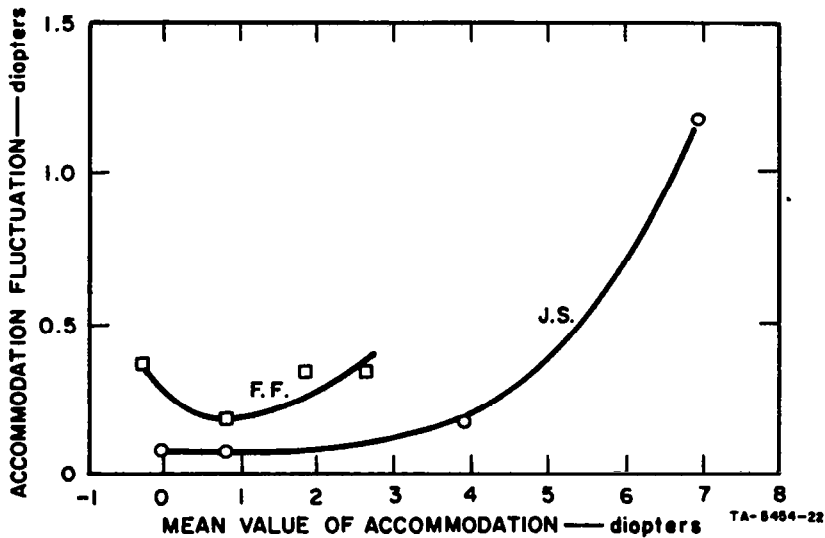


FIG. III-2 MEAN VALUE OF ACCOMMODATION FLUCTUATIONS AS A FUNCTION OF THE AVERAGE VALUE OF ACCOMMODATION

Source: Arnulf and Dupuy (1960)

4. Using two continuous-recording optometers it was found that time plots of focal variation are highly correlated in both eyes (Campbell, 1960, p. 738).
5. Campbell (1960, p. 738) showed that the amplitude of oscillation was not significantly different with monocular and binocular viewing.
6. If the position of an object is vibrated axially along the visual axis, the spectral plot shows the position of the spectral peak shifting to exactly match the frequency of the object movement. This tracking occurs at least between $\frac{1}{2}$ and 3 cps. The accommodation tracking response, in other words, is not in addition to the nominal 2 cps peak, but rather the peak shifts so that only a single peak appears in the spectral plot. Campbell, Robson, and Westheimer (1959, p. 587) report an average response delay of about 0.4 sec independent of frequency.
7. Drugs, such as homatropine, which anesthetize the ciliary muscle, also eliminate the vibration component.
8. Arnulf and Dupuy (1960) apparently found a rather large component of astigmatic variation in these vibrations. This adds other possibilities in focus control, and is commented on further in Sec. III-F.

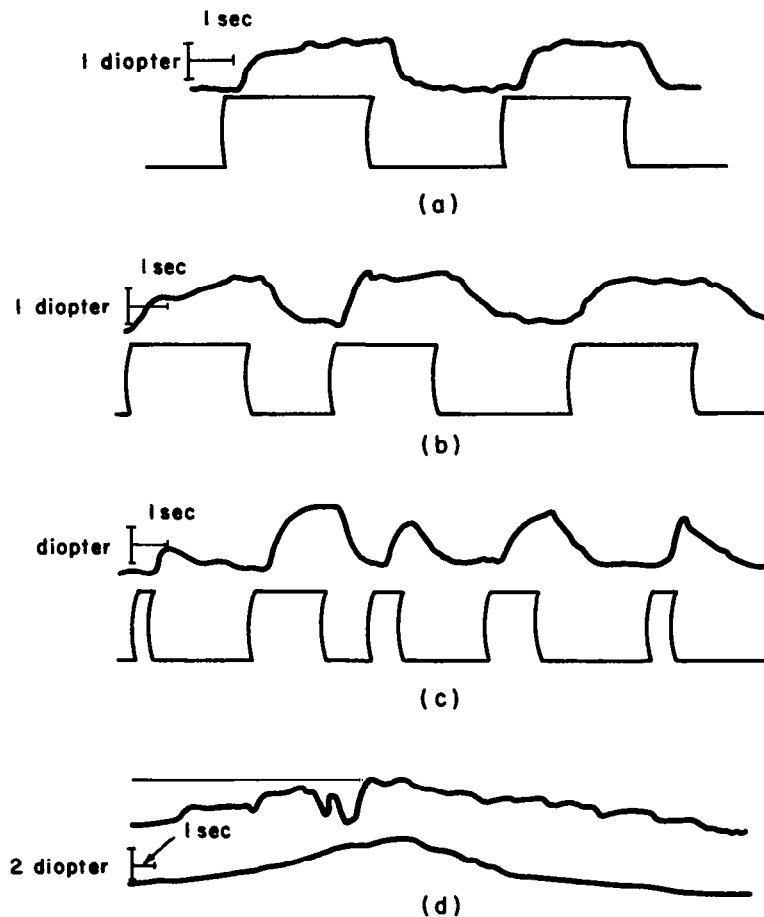
C. Reaction Time

According to Campbell and Westheimer's results (1960), reaction time for a far-to-near response is 0.36 ± 0.09 msec, and for a near-to-far response is almost identical at 0.38 ± 0.08 msec. (Reaction time is measured as the interval between stimulus change and the start of an accommodation correction.) Typical responses are shown in Fig. III-3(a). The response itself may last 0.6 sec or more, and sometimes much longer.

This is a very long reaction time. Alpern (in Davson, Vol III, p. 192) notes that the accommodation reaction time is three times as long as the shortest reaction time for a saccadic shift of gaze between two objects at the same distance from the eyes. It is almost twice as long as the reaction time of a fusional vergence movement. Campbell and Westheimer (1960, p. 292) noted that the pupil response associated with an accommodation correction (part of the "near reflex") is also long. In one particular result in which accommodation reaction time was 0.30 sec, pupil reaction time was 0.32 sec. This compares with a pupil reflex to simple light intensity change of about 0.24 sec.

Campbell and Westheimer show accommodation responses to sinusoidal stimuli, pulse stimuli, and slow ramp stimuli (1960). An interesting result regarding a step change in object distance, without the normal accompanying change in image size, is that the response was not smooth, but consisted of a number of step-like responses separated by time intervals of the order of a reaction time, Fig. III-3(b). (This condition is achieved with an optical arrangement in which the effective size of the target alters with changing distance so as to maintain a constant angular size.)

If the accommodation reaction time of about 0.39 sec is "three times that of a saccadic movement," this means that it is about 250 msec longer, and 250 msec is exactly a half period of a 2 cps wave. Could we use this as an argument for a relevant role of the vibration? We pursue this point further.



TA-6454-27

FIG. III-3 RECORDS OF ACCOMMODATION RESPONSES

- (a) Responses to a 2 diopter step stimulus and return to zero level of accommodation. Upward movement represents far-to-near accommodation. This record is an example of single-sweep accommodation response.
- (b) Typical responses to a 2 diopter step stimulus and return when targets change only in focus and not in size.
- (c) Responses when a far visual stimulus is replaced by an identical one at a nearer optical distance for various time intervals presented in random order (rectangular pulse stimuli)
- (d) Response as a target's optical distance is gradually changed

Source: Campbell and Westheimer (1960)

D. Conscious Perception of Blur

Campbell and Westheimer (1958, p. 18), using a 3 mm artificial pupil and a high contrast object on a white background tried to find the sensitivity to blur as a function of defocus amplitude. Their results are shown in Fig. III-4. In this experiment, the object distance is vibrated at 2 cps about an average position, the amplitude of vibration being under control of the subject. Along the abscissa is plotted the average magnitude of defocus. The ordinate records the amplitude

of sinusoidal distance vibration at which the subject could just consciously perceive some change over the cycle. Note that the subject could tolerate much larger vibration amplitude with optimum focus. This is explainable in terms of the spread function of light.

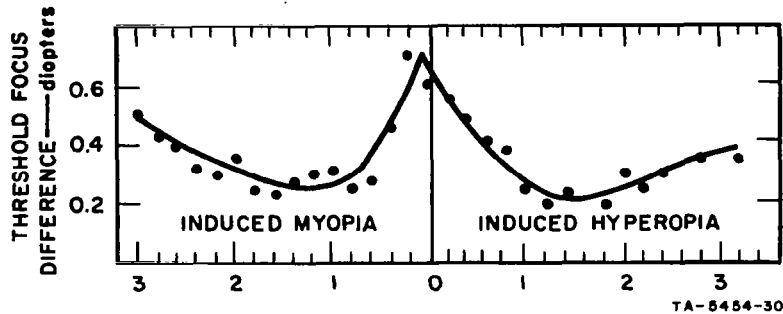


FIG. III-4 THRESHOLD AMPLITUDE OF SINUSOIDAL DISTANCE VIBRATION TO DETECT BLUR AS A FUNCTION OF DIFFERENT AVERAGE VALUES OF DEFOCUS

Source: Campbell and Westheimer (1958)

Westheimer (1963, p. 92) using a 3 mm pupil, and with the eye at best focus, estimated the spread function to be that shown in Fig. III-5, which shows the transverse intensity distribution of a fine-line image on the retina in best focus. Their measurements showed that the spread function with a 6 mm pupil and best focus is just slightly worse than for the 3 mm case.

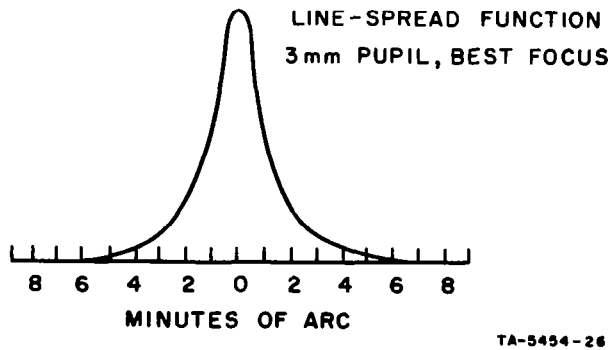
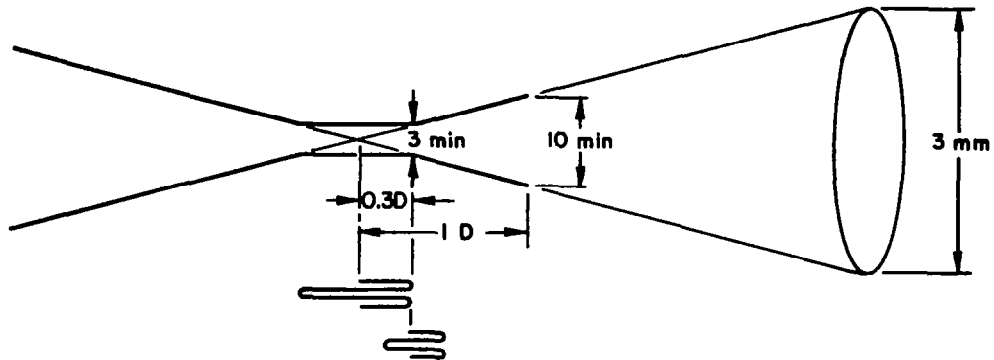


FIG. III-5 LINE-SPREAD FUNCTION IN LIVING HUMAN EYE FROM MEASUREMENTS OF REFLECTED AERIAL IMAGE OF LINE FILAMENT

Source: Westheimer (1963)

Using this spread function we can sketch the imaging of a point object as in Fig. III-6. For a 3 mm pupil, a 1 diopter focal change (out of a total refraction of about 60 diopters) will lead to a blur disk of $1/60$ of 3 mm, or about $10'$ of arc, as indicated in the figure. If we assume



TA-5454-7

FIG. III-6 GEOMETRY OF FOCUS FOR A POINT OBJECT, INCLUDING APPROXIMATION TO ACCOUNT FOR SPREAD FUNCTION

Source: Campbell (1954)

the spread function to have an effective diameter of about $3'$, then we would expect a relatively constant blur diameter of about $3'$ over a range from $+0.3$ diopters to -0.3 diopters. Thus, it is not surprising to find a tolerable vibration amplitude on the order of 0.6 diopters about optimum focus. (Campbell and Westheimer do not record whether the ordinate is the peak value or peak-to-peak value.) Vibrating about an average defocus of about 0.3 diopters, however, we would expect a decrease in tolerable amplitude, since there would tend to be an image variation on each half cycle of vibration.

No further comment can be made here regarding the monotonic decrease in amplitude in Fig. III-5 up to a defocus amplitude of a diopter or so, since the authors do not note just what form of object pattern was used. The result would be reasonable, however, say for a bar pattern. Following the discussion of Appendix I, we see that the critical cross-over point A for a bar would occur at a defocus of about one diopter for the case of a 3 mm lens and $10'$ bar pattern. We would suspect great sensitivity in the region of the cross-over point, which in some respects represents a pseudo point, or rather thin-line focus; for a given percent axial change there is a large percent change centered about the plane containing Point A.

E. Discussion of Vibration Role

The presence of a 2 cps accommodation vibration was initially interesting from two points of view; first, that it might offer an explanation for detection of the polarity of focus error, and second that it might explain at least part of the very long reaction time (in terms of having to correlate the signal over a significant portion of the cycle—i.e. in connection with Fig. III-6, to determine the input-output phase relation, or the relation to the central flat zone.) We have since conceived of a third possible function, which has to do with increasing the effective depth of field (this possibility is discussed in Appendix II). At this time, however, none of these roles has been

completely verified. Although the theoretical models developed later in the report lead to a new hypothesis regarding the source of these vibrations, the models do not provide any new method of interpreting existing data to verify the role of vibration. It is hoped, however, that the new experiments suggested by these models will help develop more definite answers.

We might note that Stark (1965, p. 65) has completely written off any vibration role. He comments

“... no better than chance results were obtained; thus providing direct experimental evidence against this mechanism for phase-sensitive detection to obtain an odd-error signal. These oscillations must rather be viewed as a non-functional indicator of the nonlinear characteristics of the accommodative servomechanism described in the preceding paper.”

He draws this conclusion primarily because under certain conditions of step changes in target distance, he found that subjects operated at about the 50 percent level (i.e., essentially randomly) with regard to the initial direction of accommodation correction. They apparently were not able, in other words, to determine polarity of accommodation error on the basis of phase. We do not feel that we can write the oscillation off too quickly, however, because in terms of the processing models developed later in the report, we might well expect significant difference in performance with large and small step changes in target distance, with the transition occurring in the 1 to 2 diopter range. In Stark's experiments, he typically reports ± 2 diopter step changes. The subject of incorrect initial response is discussed further in Sec. VII-D.

Another point regarding the lens vibration is in connection with dynamic astigmatic effects. The annulus-shaped ciliary muscle is innervated by a number of different sections of nerve radiating from the penetration point of the optic nerve through the retina. Though the control system may be such that the pull from each section is equalized to minimize astigmatism in steady-state, any significant difference in reaction time of the various muscle sections would lead to at least a transient astigmatism. A 125 msec difference in the response of horizontal and vertical sections, for example, would result in a 90° time difference and therefore to a smooth rotational astigmatism effect. (Arnulf and Dupuy (1960) report that accommodation vibrations are in fact mainly astigmatic.) This too leads to interesting possibilities for focus control, though we have insufficient data to pursue this topic in any greater detail. For comment on application of rotational effects in pattern processing see Bliss and Crane (1964), though discussion in this reference is in terms of a rotating lens slit, the arguments are readily adapted to the case of a rotating cylindrical lens.

A point of interest is the concentric ring illusion of Helmholtz. In this illusion there seems to be a rotational sensation of a number of radial zones in the pattern. MacKay (1958, p. 362) suggested that the illusion is really a Moire pattern effect, due to superimposing of the pattern on recent after-images of the same pattern at slightly different locations. Campbell and Westheimer (1958, p. 362) suggest, however, that it is due to the accommodation vibration, since when focused at infinity, or with a small artificial pupil, or with homatropine, the illusion disappears. These are all conditions in which the vibration amplitude becomes negligible. The rotational effect of the illusion is interesting in connection with any hypothesis regarding the rotational astigmatic effect of the rotation.

IV IMAGE PROCESSING BASED ON NONLINEAR RECEPTORS

As for image processing, we derived a technique in Sec. II that worked well, at least for nonlinear photocells. In this section, we try to evaluate the role of the nonlinear retinal cells in a similar wide-area, nonlinear photocell role. We conclude that this technique is not a likely candidate to explain actual accommodation control, although we cannot be sure that it is not in at least some way involved. Starting in Sec. V, we develop a different image processing model that seems far more appealing.

A. Receptor Cell Nonlinearity

For our purposes now, let us assume that the central retinal region of, say, 30' diameter, is made up of identical nonlinear receptor cells whose outputs are linearly summed, in the manner of Eq. (II-1). It is typically reported that the basic cell response is approximately logarithmic over a relatively wide range of light intensity. However, the analysis is simpler for exponential power functions, in which case the equations of Sec. II can be directly applied. Let us assume then a less strongly saturating response function of the power type. In particular, let us assume that the basic response is of the form

$$g = kI^{1/2}; \quad (IV-1)$$

i.e., $p = 1/2$ in Eq. (II-3)

B. Small Object; Point Source

Assume that a point object is brought to focus in the center of the receptor area. We wish to determine the $G(z)$ curve in the manner of Fig. II-3. In the present case, we will measure z in diopters and G will be a measure of the output function, not conductance as in the case of the photocell. Changes in focus due to any cause are shown in terms of an equivalent retinal movement, for ease of illustration.

For small magnitudes of defocus, the point pattern remains completely contained on the finite receptor sheet. Assuming an ideal point image in focus, we can directly apply Eq. (II-6), inserting for p the assumed value $1/2$. Thus, we have

$$G = k_1 |z|; \quad (IV-2)$$

that is, G is a linear function of defocus magnitude.

The image, if initially centered, remains completely contained on the receptor sheet up to Position C in Fig. IV-1(a). Beyond that, e.g. in the region of position D , the function changes because the defocused image is now larger than the receptor area. The resulting functional form is

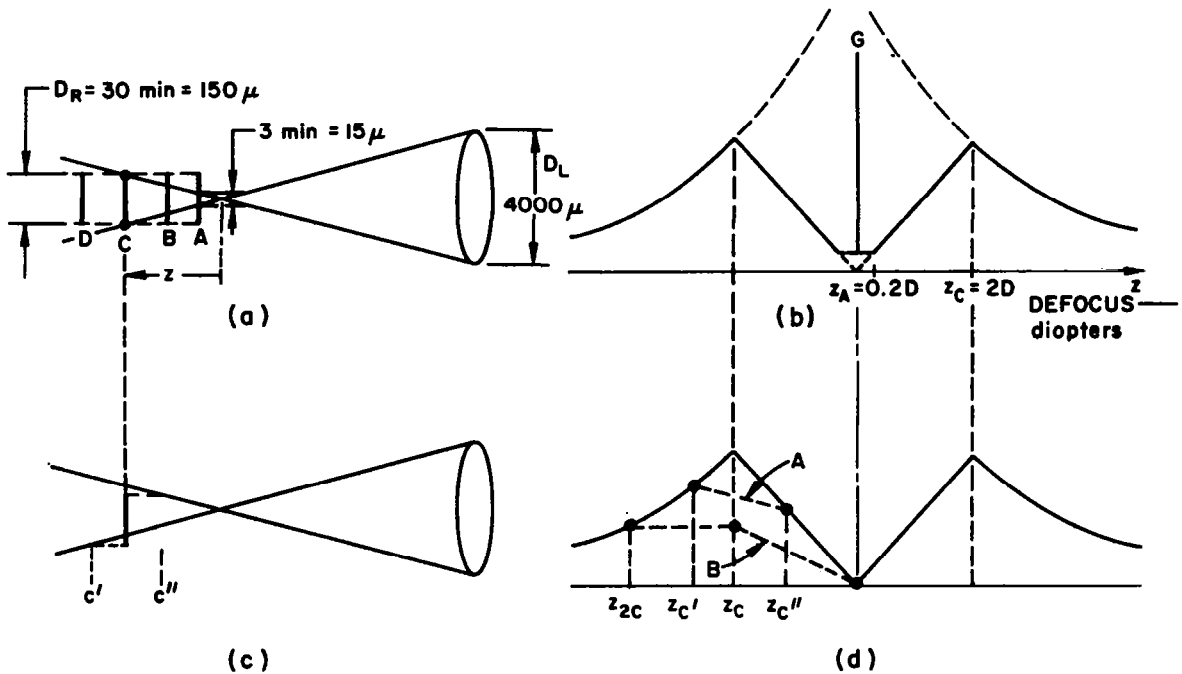
$$G = \frac{k_2}{z}; \quad (IV-3)$$

that is, a hyperbolic relation, as shown in Fig. IV-1(b). The cross-over point z_c is the magnitude of defocus that makes the blur circle just equal to the receptive diameter. This is assumed to be

30' of arc, or 150μ (assuming 1' of arc corresponds approximately to 5μ on the retina). By simple geometry, we see that z_c is closely approximated by

$$z_c = (D_R/D_L)F, \quad (IV-4)$$

where D_R is the receptor field diameter, D_L is the pupil diameter, and F is the total refraction. For $D_L=4$ mm and $F=60$ diopters, $z_c \approx 2$ diopters. For a larger pupil, or smaller effective receptor field diameter, the critical defocus distance would be smaller. Assuming a point spread width of about 3', the magnitude of defocus to reach Position A is approximately 0.2 diopters.



TA-5434-4

FIG. IV-1 $G(z)$ CURVES FOR DIFFERENT LOCATIONS OF A POINT SOURCE ON A FINITE RECEPTOR FIELD
 (a) Centrally located
 (b) Off-center

Erroneous Response. The compound curve of Fig. IV-1(b) has certain interesting features. For small vibrations about an average defocus less than 1 to 2 diopters, the phase of the output signal with respect to the lens vibration could readily determine the polarity of defocus, as discussed previously. But beyond z_c the phase reverses. Thus, using phase to determine direction of error with this type of processing could actually give wrong results for large defocus.

Another point of interest is the fact that there are three regions of zero slope in Fig. IV-1(b). If optimum focus is nominally obtained in terms of reaching a zero slope region (generally about $z=0$), then the system could possibly stabilize at incorrect zero slope positions.

Off-Center Image. The curve of Fig. IV-1(b) was derived on the basis of a point-source object exactly centered on the receptor region. In the course of fixation, however, we know that

the image wanders considerably. Let us consider how the curve changes with lateral movement of the image over the receptor region.

If the receptor field is lower, so that at Position C it is as indicated in Fig. IV-1(c), then to the right of Position C'' and to the left of Position C' , the $G(z)$ curve is the same as for the centered image. (Position C' is as far to the left as Position C'' is to the right of Position C .) Between Positions C' and C'' there is a connecting curve labeled A in Fig. IV-1(d).

If the in-focus point source is located exactly at the edge of the receptor field, and if we assume a square-shaped lens and square-shaped receptor area, then the "connecting curve" has exactly half the slope of the original linear curve (curve labeled B in Fig. IV-1(d).) Beyond Position C the curve is flat until it reaches the hyperbolic region. The reason for the flat region is that between C and $2C$ (i.e. twice the distance to C) the net area increases linearly with z ; to the right of C the area grows as z^2 to the left of $2C$ the area is constant.

If the initial in-focus point is beyond the edge of the receptor field, then the $G(z)$ curve is of course flat for some region on either side of $z=0$.

C. Discussion

With point images completely contained within the small receptor field, we see that we could obtain some suitable control information simply by linearly summing the outputs of individual, nonlinear receptor cells. At least for small magnitudes of defocus the polarity of response according to Fig. IV-1(b) could guide the focus control in the proper direction toward $z=0$. However, we see also the possibility of wrong polarity of response for too large a defocus step, and we find other potential stable points.

The success of simply summing the outputs of individual nonlinear cells depends upon having very uniform receptor response, and upon the total light in the field remaining sufficiently constant so that changes in total illumination do not cancel the relatively small effects from the changes in light distribution. The latter condition is especially difficult to maintain with large objects. Consider an extended contrast edge crossing the finite receptor field. If there were no lateral displacement as focus varied, the total light falling on the field would remain substantially constant. With any lateral shift in position, however, there would be significant change in total light; an increase in total light with a shift in one direction and a decrease in total light with a shift in the other direction.

Although it is instructive to see that such a simple summation of individual receptor outputs could, in principle, yield proper control information, it seems highly unlikely then that such a simple circuit approach is all that is involved in visual accommodation control, and for this reason we do not pursue the analysis for more complex image patterns. If this method is in fact used, it seems likely that it could be useful only for images which are small compared with the hypothetical size of the receptor field. We would have to conclude that the system would be relatively useless for larger patterns. Should our assumption of a small receptive field prove erroneous, then we would still be faced with the need for considerable receptor uniformity over a large field, and this is equally unappealing.

In view of these conclusions, it is important to look for other image processing possibilities. In particular, we are led to search for processing based on spatial derivatives of the light pattern. This is the topic of the following section.

V IMAGE PROCESSING BASED ON TOTAL SPATIAL DERIVATIVE

A. Discussion

In the previous section, we found that a linear summation of the outputs of nonlinear cells dispersed over a confined receptor region would be of only limited usefulness in general focus control. We would like now to investigate the role of spatial derivatives of the input light pattern. Since the effects of blurring and defocus are to reduce the high-frequency spatial components in an image, processing based on spatial derivatives seems reasonable.

In the two following sections we will discuss some interesting results of Campbell, in which he determines light-thresholds for automatic accommodation response with a large range of object size and a large range of defocus. We will show that a model based on the assumption of a limited foveal region and two-dimensional summation of the magnitude of two-dimensional spatial derivative over this surface leads to remarkably good prediction of the form of Campbell's results.

We will see, however, that this model cannot explain fine-focus control. A model based on peak amplitude of the spatial derivative field is then shown (in Sec. VII) to be more consistent with both the gross details and fine-focus requirements. Although the latter model is the more interesting at the moment, the exercise of explaining Campbell's light-threshold results on the basis of both models is instructive since a certain interesting feature of the result is explained completely differently in the two models.

In this section we assume the availability of processing circuitry to obtain pure spatial derivatives. (In Sec. VI we discuss the possibility of obtaining spatial derivatives with neural circuitry.) To be definite, we assume a first spatial derivative over the receptive field. The relevant measure is the integral of the absolute magnitude of the derivative over the entire field. Suppose, for example, that a defocused edge falls across the field. Then the derivative will everywhere have the same polarity, and the integral of the derivative over the field will (except for an arbitrary constant) simply be equal to the total light intensity. If instead of a single edge, however, we focused a bar across the field, then the derivative would have opposite polarity at the two edges, and integrating the absolute magnitude would result in a "measure of derivative over the field" that would be twice the value obtained with only a single edge.

The interesting predictive value of this model depends on the finite size of the receptor field, again assumed to be 30' in diameter. The width of a blurred edge reaches 30' of arc for surprisingly small magnitudes of defocus. Because of the truncated integration when the edge is actually wider than the receptive field, the integral of the derivative is no longer simply related to the total light intensity. It is precisely this variation in the integral which can explain the large range of data.

In this section we will use the following quantitative assumptions:

- a) an average refraction of 60 diopters
- b) an average lens-to-retina distance of 17 mm
- c) that 1' of arc corresponds to 5μ on the retina
- d) an average pupil diameter of 8 mm.

B. Light Intensity Threshold as a Function of Pattern Size

Campbell (1954) performed a simple and clever set of experiments to determine the effect of pattern size on the minimum illumination required to elicit an accommodation response. His results are summarized in Fig. V-1. In these experiments a circular disk, uniformly illuminated and of varying diameter, is placed far from the subject. The plot in Fig. V-1 shows the minimum illuminance of the disk required to elicit an accommodation response to a -3 diopter lens rapidly inserted in front of the eye after the subject was focused on the disk.

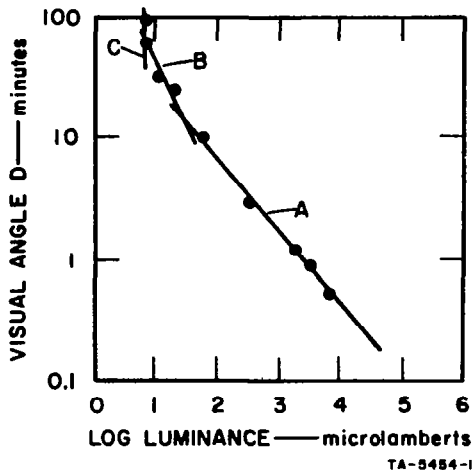
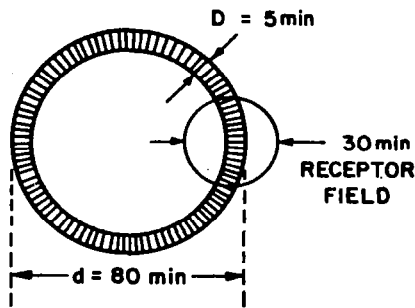


FIG. V-1 RELATIONSHIP BETWEEN TEST OBJECT SIZE AND THRESHOLD LUMINANCE FOR ACCOMMODATION REFLEX. A, B, and C represent predicted functional relations according to our model, for three different ranges of object size.
Source: Campbell (1954)

To calculate the profile of a blurred edge, it is only necessary to integrate at each point the total contribution from all possible blur disks. The result for the particular case of a uniformly illuminated circular disk and circular lens aperture is discussed in Appendix I. Let us see how those general results apply to our specific case.

For an overall refraction of 60 diopters, a 3 diopter defocus represents a shift in image distance of approximately 1 part in 20. This amount of defocus results in a blur disk diameter equal to $1/20$ of the pupil diameter. Campbell does not state the size of the pupil, but all of his experiments were performed with dark-adapted subjects, so let us assume a wide-open pupil, say 8 mm. In this case, the blur circle is 400μ in diameter, or about $80'$ of arc. In terms of the notation of Appendix I, $d \approx 80'$, which is a relatively large disk on the retina.

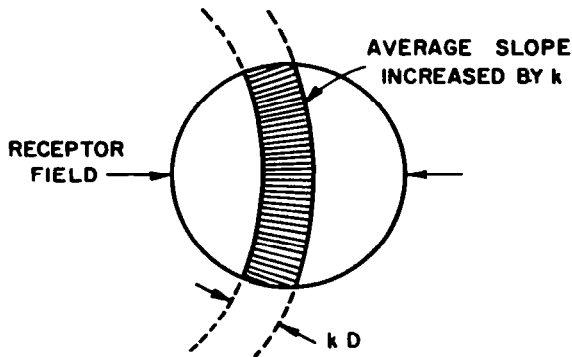
Consider the cases in Fig. V-1 for which D , the diameter of the disk object, is much less than d , the blur circle diameter. For example, for an input disk $D=5'$ the analysis of Appendix I predicts an overall retinal pattern as suggested in Fig. V-2. There is a relatively uniform central region of width $d \approx 80'$ with sloping edges of width $D \approx 5'$. Now in terms of our present model, in which focus is measured in terms of spatial derivatives, it is clear that at least some region of the transition edge must fall on the central receptive zone. But because of the large size of the defocus annulus, it is clear that only a small portion of the edge can fall on the receptive field at any instant, as indicated in Fig. V-2. Let us consider the effect of this small overlap of blurred image and receptive field. (If the blur figure were initially positioned so that no edge crossed the receptor region, we would have to postulate an eye movement before accommodation correction could occur. Interaction between eye movements and accommodation is considered more generally in Sec. IX.)



TA-8454-2

FIG. V-2 BLUR IMAGE FOR A 5 FT. DISK, 3 DIOPTERS OUT OF FOCUS, ASSUMING AN 8 mm PUPIL. The 30 ft. disk is the assumed foveal receptor region.

Consider the effect of a change in object size D . For $D < d$, the analysis in Appendix I shows that if D is scaled according to kD , where k is a constant, then the width of the transition edge increases by k , as suggested in Fig. V-3, and the height (i.e., the intensity) of the central region increases by k^2 . Thus, the average edge slope increases by k^2/k , or k , and the area containing this increased slope is also k times as wide. Therefore, the summation of first derivative over the entire foveal region will increase by k^2 ; that is, the output signal according to our model will increase by k^2 .



TA-8454-3

FIG. V-3 EFFECT OF SCALING OBJECT SIZE BY A CONSTANT k

If we now postulate some minimum magnitude of signal required for proper accommodation control then we could expect that the required threshold illumination will decrease by k^2 over this range of object size, which the results of Fig. V-1 seem to bear out. For $D < 10'$ in Fig. V-1 we see that the slope is such that a 1 log unit increase in D results in almost a 2 log unit decrease in required illumination. Of course, we must not take these numbers too literally because we do not know just what pattern measures are actually taken, or threshold effects, or the effect of non-uniform foveal circuits, and so on. The most we can hope for here is a sense of trends and consistency.

Campbell remarks that the form of the curve in Fig. V-1 seems to change in the region of $10'$ of arc. We can see the basis for Campbell assuming a change in this region in terms of our sketched lines labeled A and B . Let us consider the range represented by line B and show that such a change is consistent with our immediately preceding arguments. Note that as D reaches the same size as the sensitive foveal region, namely $30'$, the net gain in total derivative increases only as k , and not k^2 , because there is no longer any effective widening of the edge zone (as far as the receptive region is concerned) and only the increase in average slope, namely the factor k , is effective. We see in fact that the line B (drawn by eye to fit the data points in this region) has a slope almost twice that of line A .

On the basis of a rounded receptor region, we would expect a smooth transition from the k^2 mode for small D to the k mode for $D > 30'$; perhaps in the region $20' < D < 30'$. Campbell's estimate of a change occurring in the vicinity of $D = 10'$ seems too low even from his own sketched curve. A somewhat higher value on the order of $D = 20'$ seems closer.

What happens as D increases still further? In the Appendix I analysis we note a crossover at $D = d$. For $D > d$, both height and width of the edge remain fixed and only the details of the edge profile change. In other words, for $D > d$ the average slope remains constant as D increases. On the basis of our assumption of an 8 mm pupil, we saw earlier that the blur circle for a 3 diopter defocus was $80'$ of arc. With a focus measure dependent simply on the total first derivative over the field, we should then expect the threshold illumination to remain essentially fixed for $D > 80'$. The data are far too sparse to suggest that this result is actually achieved. However on the basis of the results for the two largest object sizes, namely $60'$ and $90'$, we have sketched line C which suggests a relatively constant illumination threshold, the break occurring in the region of $80'$.

Campbell, in his original paper, (1954) sketches a smooth curved line through the data points. It is interesting, however, that simply by assuming a finite receptor area and a focus measure based on summation of slopes over the field, we can define three separate ranges of object size, each with a different functional relationship, that fit the data well (as indicated by our three sketched lines A, B and C). These results tend to strengthen our working hypotheses regarding a small central receptor field and reliance on edge slope as being an important part of the focus measure.

Let us now show how this same model is consistent with another interesting result of Campbell.

C. Light Intensity Threshold as a Function of Defocus Magnitude

For a fixed target size, namely a $60'$ disk, Campbell also found the threshold intensity for different magnitudes of defocus induced by lenses inserted in front of the eye. His results for four cases are shown in Fig. V-4. Campbell sketches a straight line through these points. However, pursuing an analysis similar to the preceding one, we again find three different regions of response with functional changes occurring at lens powers of about 1 diopter and 2.2 diopters.

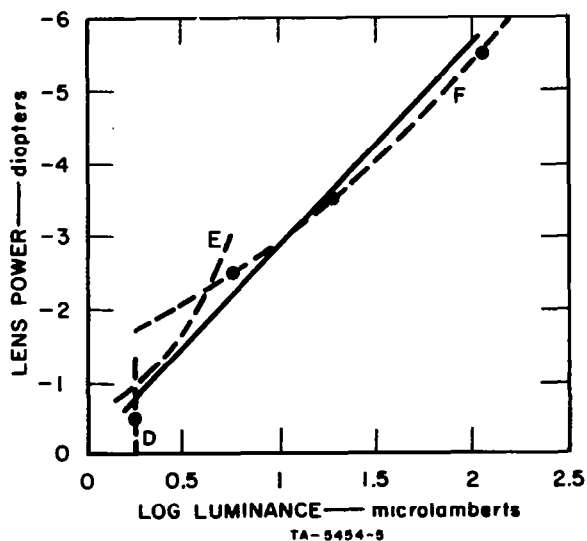


FIG. V-4 EFFECT OF POWER OF NEGATIVE LENS USED TO INDUCE ACCOMMODATION ON THRESHOLD LUMINANCE FOR THE REFLEX FOR A 1° TEST OBJECT. D, E, and F represent predicted functional relations according to our model, for three different ranges of defocus. Source: Campbell (1954)

The relevant optical configuration is sketched in Fig. V-5. In focus, we have a $60'$, or approximately 300μ circular disk image. We again assume a pupil opening, or effective lens size, of 8 mm. The defocus plane for which $D \approx d$ occurs where the two extreme rays R_1 and R_2 intersect, at the point labeled A . (We are assuming again that defocus is obtained by moving the retina but keeping the lens fixed, since this is simpler to draw.) The magnitude of defocus corresponding to Point A is approximately $(300/8,000)$ of 60 diopters, or about 2.2 diopters.

The width of the blurred edge at any location is indicated by the shading in Fig. V-5. For defocus magnitude less than 2.2 diopters, the width of the edge increases linearly with magnitude of defocus, but the intensity of the central region remains substantially constant. For defocus magnitudes greater than 2.2 diopters, the width of the edge remains substantially constant, but the intensity of the central region falls as the square of the defocus magnitude. Thus, for defocus <2.2 diopters the average slope decreases linearly with increase in defocus. For magnitudes >2.2 diopters the average slope decreases with the square of the defocus magnitude. (The edge has a width of $30'$, the assumed width of the receptor region, for about 1 diopter defocus.)

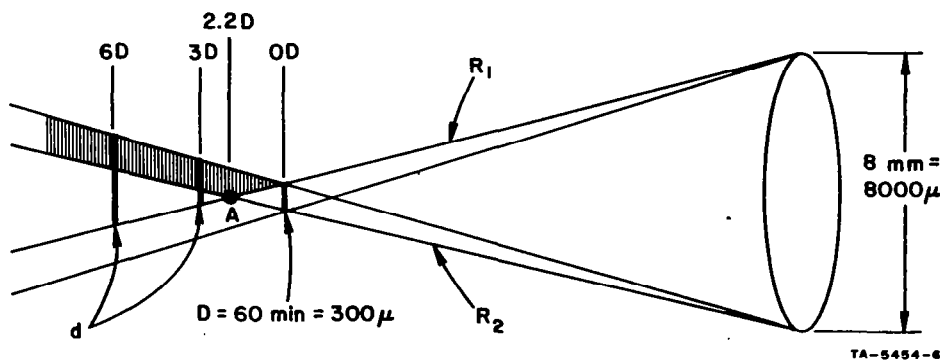


FIG. V-5 OPTICAL CONFIGURATION FOR A 60 FT. TARGET, 8mm LENS, AND AVERAGE TOTAL REFRACTION OF ABOUT 60 DIOPTERS

On the basis of these conclusions, we can sketch the three line segments labeled D , E , and F in Fig. V-4. The vertical line D indicates small expected change in threshold for less than 1 diopter defocus. This line is drawn through the only available data point in the vicinity; line F is simply drawn through the other three data points. We argued for a change in mode in the vicinity of about 2.2 diopters. Between the point defined by Line F and the 2.2 diopter level, and the point defined by Line D and the 1 diopter level, we sketch the curve E . This turns out to be a reasonable approximation to the faster variation expected in this range compared with the range beyond 2.2 diopters. We again cannot take our numbers too seriously, especially in view of the very sparse data points. One might at least be tempted to suggest that the three upper data points lie on a different segment of curve than the lowest point. It would be interesting to rerun such a curve with more data points.

D. Limitations of the Model

We have considered a processing model based on summing the absolute magnitude of first (spatial) derivative over a receptive field. The model fits Campbell's results reasonably well over a wide range, except for relatively small magnitudes of defocus, i.e. fine-focus control. The

problem is that with small defocus the entire width of the blurred edge fits on the receptive area, as in Fig. V-3, in which case summation of the derivative is independent of width. It was this condition that led to hypothesizing the vertical segment D in Fig. V-4.

Thus, we have a good start at a processing model, but some alteration is required to provide for fine-focus control. In the next section we will consider how spatial derivatives may be obtained with neural circuitry. The result is not a pure spatial derivative in the sense considered here. The derivation will point to a modification of our processing model which involves more a measure of the peak magnitude of spatial derivative over the field than simply a total summation of derivative. We will see that a model based on peak detection not only fits Campbell's results, but can provide for fine-focus control as well.

VI SPATIAL DERIVATIVES BY NEURAL CIRCUITRY

A. Lateral Inhibition

It is well-known that lateral inhibition in a two-dimensional array provides an output component resembling a second spatial derivative. This result is often discussed under the subject of edge sharpening, or Mach bands. For an up-to-date account of the history and work in this field, the reader is referred to the very interesting book on Mach Bands by Ratliff (1965). We treat the subject here in just sufficient depth to draw certain conclusions for our models.

A one-dimensional lateral inhibition network is illustrated in Fig. VI-1, where a set of cells having inputs labeled . . . a, b, c, \dots and outputs labeled . . . a', b', c', \dots are interconnected so that each input tends to directly inhibit the neighboring outputs. Let the cross-connection gain be k , and let the local input-output gain be unity. Then the output of the second cell can be expressed as

$$b' = [b - k(a + c)]. \quad (\text{VI-1})$$

For $k = 1/2$ Eq. (VI-1) takes the form

$$b' \propto [2b - (a + c)] = (b - a) - (c - b), \quad (\text{VI-2})$$

which is proportional to the second spatial difference of the input pattern at cell b . For a densely packed set of cells we can treat the output as approximating a second spatial derivative of the input pattern. The same conclusion can be shown for a backward inhibition network—i.e. an inhibitory model in which feedback is from outputs to adjacent inputs. It is simpler to demonstrate, however, with the forward connection.

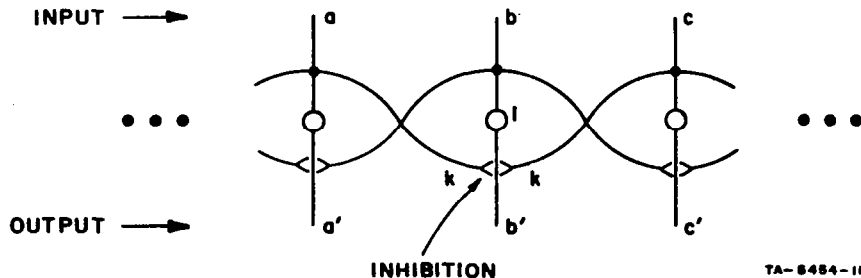


FIG. VI-1 ONE-DIMENSIONAL LATERAL INHIBITION NETWORK

With this second-derivative measure (obtained by strong lateral coupling represented by $k = 1/2$) the network output would be unresponsive (i.e. zero) for a uniform field intensity, as well as for one that exhibited a linear change of intensity with distance. With nonzero second and higher derivatives there would be a pattern to the output, with particularly high response in the region of sharp boundaries.

If the basic receptor elements are linear, however, and could (conceptually, at least) yield negative as well as positive outputs, then the earlier conclusion in Sec. IV about the ineffectiveness of simply summing receptor outputs applies even with the addition of linear lateral interconnections. By forming the linear sum of all outputs of the form of Eq. (VI-1), the net result is again simply proportional to the total light input, and independent of the distribution of light.

To be useful for processing blurred images—i.e. to be sensitive to the state of focus—we must therefore look for nonlinearities in the lateral connectives. There are two forms of nonlinearity relevant to lateral inhibition networks, apart from the basic cell nonlinearity itself. One is the threshold in the lateral connectives, which is generally reported to be a function of the length of the connective. Lateral inhibition is not simply a nearest neighbor effect, as suggested in Fig. VI-1, but each cell interconnects with many cells over a relatively large area. Thus the greater the average light intensity the greater the surrounding zone of lateral connectives that become effective. We could therefore expect the lateral effect to increase with the average intensity of the picture.

A second nonlinearity is the cut-off that occurs when the total inhibition applied to a cell is larger than the total excitation. (That is, a real cell cannot give a negative output). Thus we obtain a unipolar output pattern which is relatively large only in the vicinity of contrast changes. For example, for $k = \frac{1}{2}$ (in the one-dimensional case), the output from each cell would be zero for a uniform light field, or one varying linearly with distance. With a more highly varying field (e.g. of the form $I = kx^p$ where I is intensity and x a spatial dimension) outputs would be non-zero in regions where intensity was varying less rapidly than linearly, i.e. $p < 1$; though still zero where variations were more rapid than linear, i.e. $p > 1$

B. Neural Unit

The net effects of extended lateral interconnections, as well as extended summation effects due to input pattern “spread” (e.g. by diffraction effects in the visual optics), are often displayed in terms of a “neural unit,” of the form indicated in Fig. VI-2(a) for a rotationally sym-

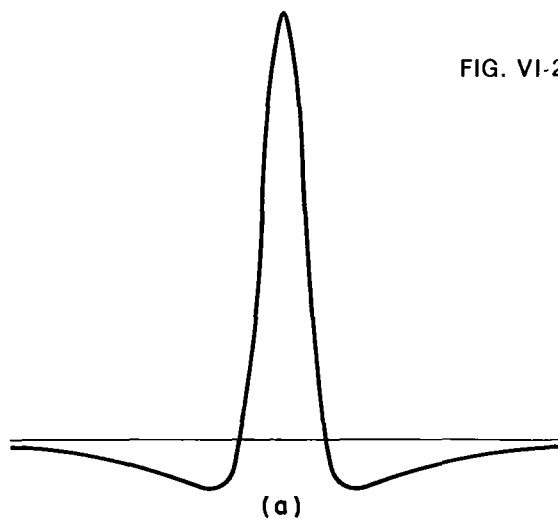
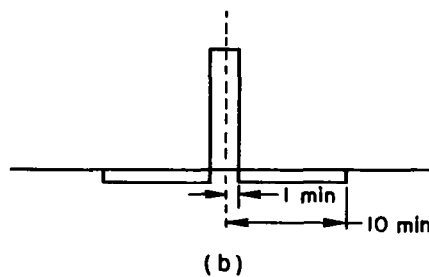


FIG. VI-2 FORM OF NEURAL UNIT
 (a) Computed from retinal transfer function
 (b) Idealized form

Source: Davidson and Cornsweet (unpublished)



TA-5454-12

metric case. The neural unit can be computed from an overall spatial transfer function for the visual system—i.e. a plot of output amplitude as a function of input frequency—but here by “frequency” we mean the spatial frequency of the input pattern. This transfer function has the form of a band pass filter function, being small at low frequencies because of lateral inhibition effects, and small at high frequencies because of diffraction effects and optical aberrations. (For an example of an overall transfer function plot see Fig. 4.9 of Ratliff, 1965.) This function peaks at a spatial frequency of about 20 cycles per millimeter on the retina, which corresponds to one cycle every 10' of arc.

The neural unit can be considered as a two-dimensional transmission mask with positive and negative values. To find the output at any point of the field, one simply overlays the two-dimensional neural unit on the input pattern (with the center of the neural unit located at the point of interest) and integrates the point-by-point product of mask and input pattern. Typical dimensions for an idealized form of neural unit in Fig. VI-2(b) are a central summation zone of 1' radius and a surrounding inhibition zone of about 10' radius.

To see the effect of neural unit processing, consider the black-white edge of Fig. VI-3, with a linear transition zone of width W . With a 4.5 mm pupil, a 1 diopter defocus (for an assumed total refraction of 60 diopters) would lead to a width $W=15'$. In general, the width would be $W=(15D)'$, where D is the magnitude of defocus in diopters. Assuming the neural unit of Fig. VI-2(a), the output patterns for various magnitudes of defocus are shown in Fig. VI-4. A plot of peak value versus magnitude of defocus is shown in Fig. VI-5. Computed output plots for sharply focused bar patterns of various widths are indicated in Fig. VI-6.

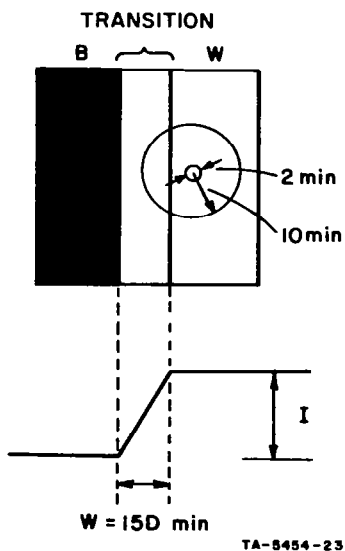
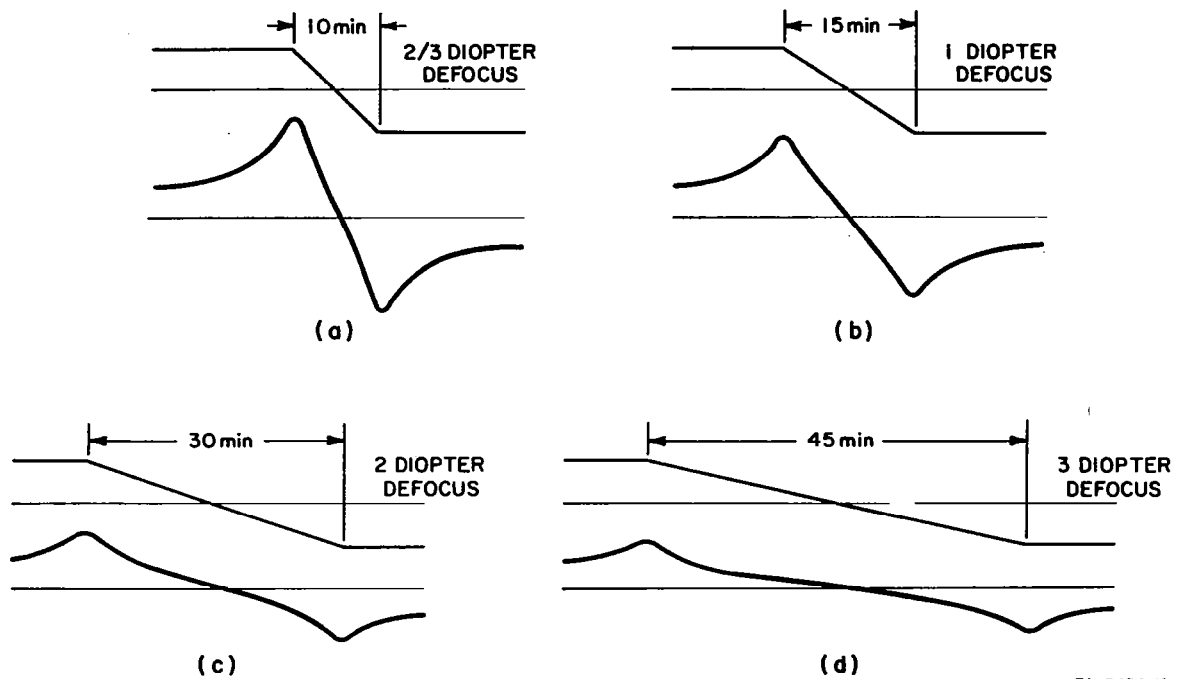


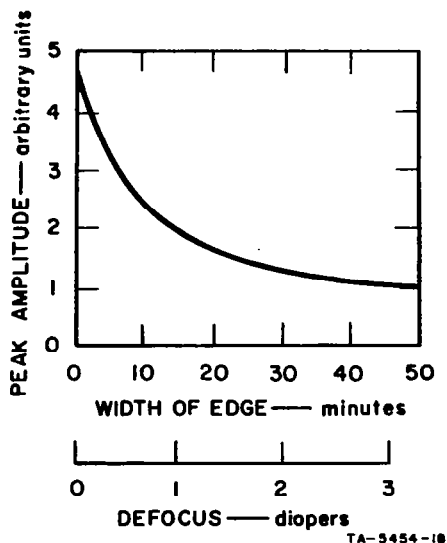
FIG. VI-3 NEURAL UNIT PROCESSING OF BLACK-WHITE TRANSITION EDGE
 D —Magnitude of defocus in diopters



TA-5454-19

FIG. VI-4 COMPUTER PLOTS OF OUTPUT FOR DEFOCUSED EDGE PATTERNS, BASED ON NEURAL UNIT PROCESSING

Source: Davidson and Cornsweet (unpublished)



TA-5454-18

FIG. VI-5 PLOT OF PEAK VALUE OF OUTPUT AS A FUNCTION OF DEFOCUSED EDGE WIDTH, FROM COMPUTER SIMULATION OF NEURAL UNIT

Corresponding magnitude of defocus shown as lower abscissa scale.

Source: Davidson and Cornsweet (unpublished)

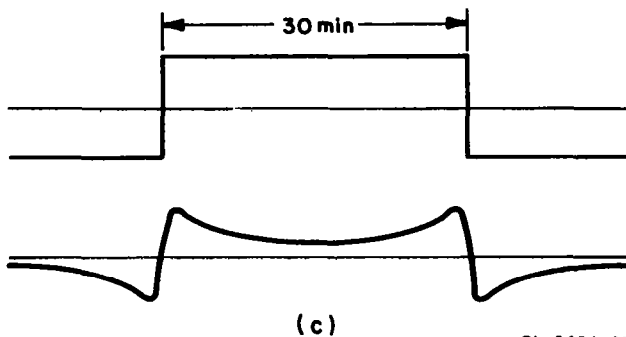
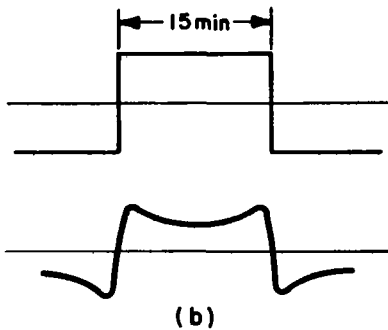
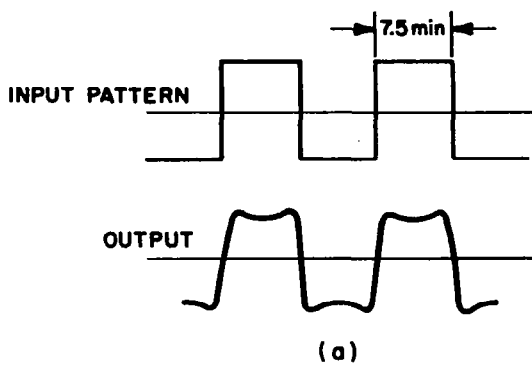


FIG. VI-6 COMPUTER PLOTS OF OUTPUT FOR VARIOUS BAR PATTERNS, BASED ON NEURAL UNIT PROCESSING
Source: Davidson and Cornsweet (unpublished)

TA-8484-20

C. Peak Detection

We see that the rather ubiquitous lateral inhibition networks can provide us with a component of spatial derivative of the input pattern, primarily a component of second spatial derivative. For purposes of our accommodation control model, we must consider how the two-dimensional derivative field is further processed to develop a final output control signal. Here we get onto unsure ground.

We might speculate on one grand ganglion element that summates over the entire field; or what seems more likely, several steps of convergence—each step again incorporating lateral inhibition connectives to sharpen the edges even further. In any case, because of non-zero thresholds in any summation mechanism we could speculate on an overall summation in which there is significantly greater weighting to the peak values of the derivative fields—particularly if there are multiple layers of neural-unit processing. In Section VII we evaluate the consequences of assuming that the net effect of the processing is only to monitor the peak values in the derivative field.

We will see that such a model is consistent with a relatively broad spectrum of experimental results, and stimulates a number of new experiments in accommodation.

D. Dynamics of Neural-Unit Processing

Before considering the peak detection model we would like to mention certain temporal aspects of lateral inhibition networks that are important to keep in mind. Because of transmission delay in the lateral connectives, the output pattern immediately after presentation of an input pattern will not yet show the effects of lateral inhibition. Crudely speaking, the output pattern is determined by the present input pattern, and by the lateral inhibition pattern a short time ago. Suppose that we have a steady input edge pattern *A*, with the resulting output pattern *A'* of Fig. VI-7. (By steady input pattern we mean one impressed long enough to establish the full strength of the lateral interconnections.)

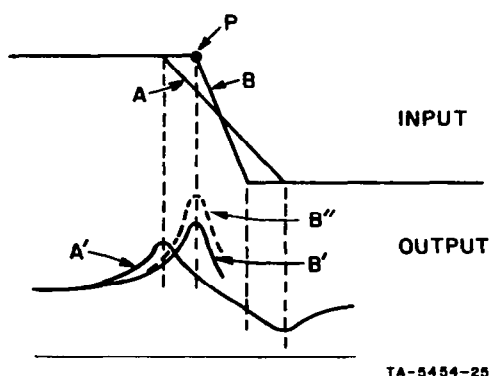


FIG. VI-7 TRANSIENTLY ENHANCED EDGE SHARPENING WITH AN ABRUPT EDGE CHANGE. Enhancement due to delay in establishing full effect of lateral inhibition.

Immediately after an abrupt sharpening of the edge to pattern *B* we would get a large transient increase in output, since the net inhibition at the new corner point *P* is even less than it will be when the new inhibition levels for the sharpened edge pattern become effective. In other words, the dynamics are such that there could be a larger transient increase in peak value than the eventual steady-state increase. This transient effect is suggested by the dashed curve *B''* in Fig. VI-7, which has a larger peak amplitude than the corresponding steady state curve *B'*.

There are also temporal effects due to spatial movement of an edge pattern over the retina. In particular, small transverse movements of a black-white edge significantly increase the sensitivity to perception of Mach bands, as suggested in Fig. VI-8. In these experiments the minimum spatial gradient for which the Mach bands are just perceptible is determined. Note the significant decrease in required gradient (i.e. increased sensitivity) by the introduction of transverse vibration. Of greatest significance to our present study is the fact that the greatest improvement in sensitivity occurs in the same frequency range as accommodation vibrations (2 to 3 cps). In this regard, we should note that the lens vibration not only causes variation in edge sharpness; but there is also an associated lateral vibration of the entire image, since the foveal axis (visual axis) is displaced from the optical axis by approximately 5°. The lateral shift associated with the vibration is discussed further in Sec. VII-C.

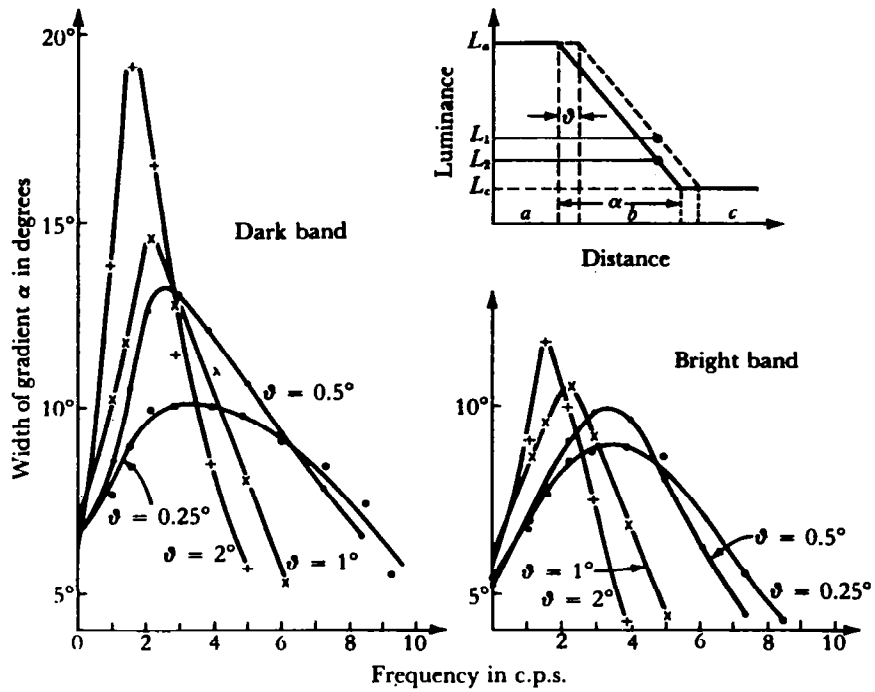


FIG. VI-8 WIDTH OF GRADIENT (α) REQUIRED FOR BANDS TO BE VISIBLE IN MACH PATTERN OSCILLATED AT VARIOUS FREQUENCIES (cps) FOR 4 DIFFERENT AMPLITUDES OF MOTION (ϕ)

Source: Ratliff (1965)

Further study of temporal effects associated with lateral inhibition networks seems very important for better evaluation of these phenomena in our accommodation model, and in visual perception in general.



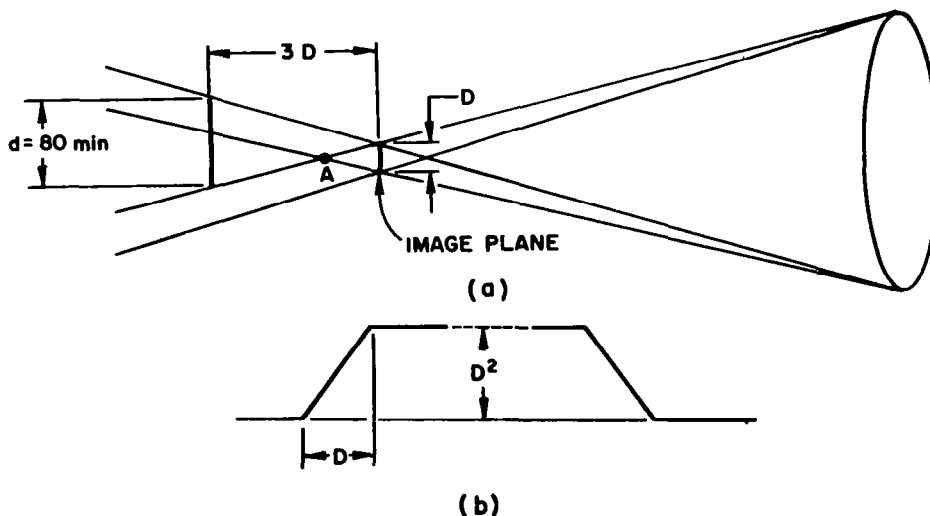
VII IMAGE PROCESSING BASED ON PEAK VALUE OF DERIVATIVE

We were able to explain Campbell's results of Figs. V-1 and V-4 with a model based on summation of the absolute magnitude of spatial derivative over the receptive field. We saw, however, that this model was not sufficiently sensitive for small magnitudes of defocus. In Sec. VI we considered neural methods of measuring derivatives and concluded that a greater weighting of the peak values of the derivative seemed reasonable. To evaluate this point further, we will investigate in this section the consequences of a model based simply on peak detection over the receptive field. We will see that this form of model is also consistent with Campbell's results, and provides a useful basis for fine-focus control as well.

A. Peak Detection Over the Field

Let us first show that a peak measure over the receptive field can also predict Campbell's results of Fig. V-1, in which threshold illumination was determined as a function of object size for a fixed defocus of 3 diopters. Recall that the blur circle for a 3 diopter defocus and a wide-open pupil (assumed to be 8 mm) is $80'$. All of the defocus patterns therefore have a relatively large diameter compared with the neural unit and compared with the presumed receptive field.

For a disk diameter $D < 80'$ the optical configuration is as shown in Fig. VII-1(a), with cross-over point A to the right of the 3-diopter defocus plane. The resulting profile in the 3-diopter plane has the form sketched in Fig. VII-1(b). The intensity of the bright center is proportional to D^2 , the edge width is essentially equal to D , and the average edge slope therefore varies as D .



TA-8484-8

FIG. VII-1 OPTICAL GEOMETRY FOR A DISK IMAGE
 (a) Configuration for an in-focus disk image of diameter D
 (b) Dependence of profile on diameter D for large defocus,
 beyond cross-over point A

In Campbell's results we note that for D less than a few minutes of arc, the functional dependence is as D^2 . This was explained in the earlier model by accounting for the width as well as the average slope of the transition edge.

In the present model the D^2 dependence for small D arises from a totally different process. From Fig. VI-5 we see only a small change in the peak value over the range from zero to just a few minutes of arc. In this range, then, the peak amplitude is mainly proportional to the height of the transition edge, so that according to Fig. VII-1 the peak amplitude output should vary as D^2 .

Over the range of D from a few minutes of arc to $20'$ of arc, however, we see a much larger change in peak amplitude with variation in width. As D increases in this range, the central intensity again varies as D^2 , but there is a counterbalancing decrease in the peak due to an increase in edge width. Thus, we would expect a gradual shift in slope towards a linear dependence on D , as we actually see in Fig. V-1.

When D reaches the magnitude of the blur circle diameter, i.e. $D=d$, we again expect the curve of Fig. V-1 to become substantially vertical since for still larger D there is relatively little change in edge shape.

Hence, we have a different explanation for Campbell's results, the change in curvature for D in the $20'$ range not being due to the limited receptor region, as before, but rather to the effects of neural-unit processing. This model fits Campbell's data of Fig. V-4 also, at least as well as the first model.

B. $G(z)$ Curves

We now have a model that can provide for fine-focus control, since the curve of Fig. VI-5, if extended to the left (i.e. for opposite polarity defocus) would similarly decrease from the peak value at zero defocus, much in the manner of $G(z)$ curves of Sec. II. Note that the curve of Fig. VI-5 would predict a relatively large change in output for a few-tenths diopter vibration, though the output variation would decrease rapidly for defocus greater than one or two diopters. Of course, the curve could not actually be as sharp at the origin as indicated, because of the limited resolution in terms of the spread function.

It would be instructive to study $G(z)$ plots of this type for different shapes and sizes of objects in order to determine, in particular, whether the peak value is a monotonic increasing function of focus for all types of patterns.

C. Lateral Movements of the Image

Two types of image movement accompany accommodation changes. One is due to shifts in the principal planes of the optical system; the second results from the nature of the lateral inhibition circuits.

Recall from Fig. VI-4 that an edge peak occurs close to the corner position of the input pattern. Thus, with a sharpening of focus from pattern A to pattern B in Fig. VII-2, there will be a relatively large lateral shift in the position of the peak. The direction of shift depends on the orientation of the edge. With high intensity on the left (as in Fig. VII-2) the shift is to the right; with high intensity on the right the shift is to the left. For a 4.5 mm pupil and 1 diopter defocus, the edge would blur over a width of approximately $4500 (1/60) \mu$, or about $15'$. Hence, from optimum focus to 1 diopter defocus we could expect a lateral shift of the edge peak by about one half this amount, or about $7.5'$.

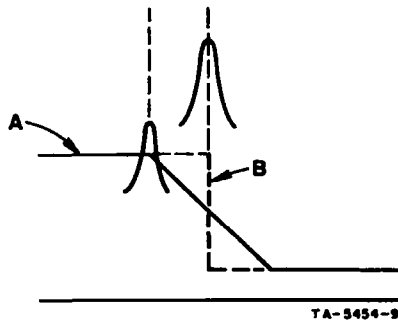


FIG. VII-2 LATERAL SHIFT OF PEAK POSITION WITH FOCUS CHANGE

Concerning shift of optical planes with change in accommodation, Southall (1961, p. 58) notes that for a 12 diopter accommodation change, the center point of an equivalent lens system (i.e. the point through which the central undeviated ray passes) shifts about 0.48 mm along the optic axis. Assuming a linear relation between magnitude of axial shift and magnitude of accommodation change, the average shift would be 0.04 mm per diopter focus change. For a 5° displacement of the visual (foveal) axis from the optic axis, we would then expect about 0.7' lateral shift of the image on the retina per diopter change, as suggested in Fig. VII-3.

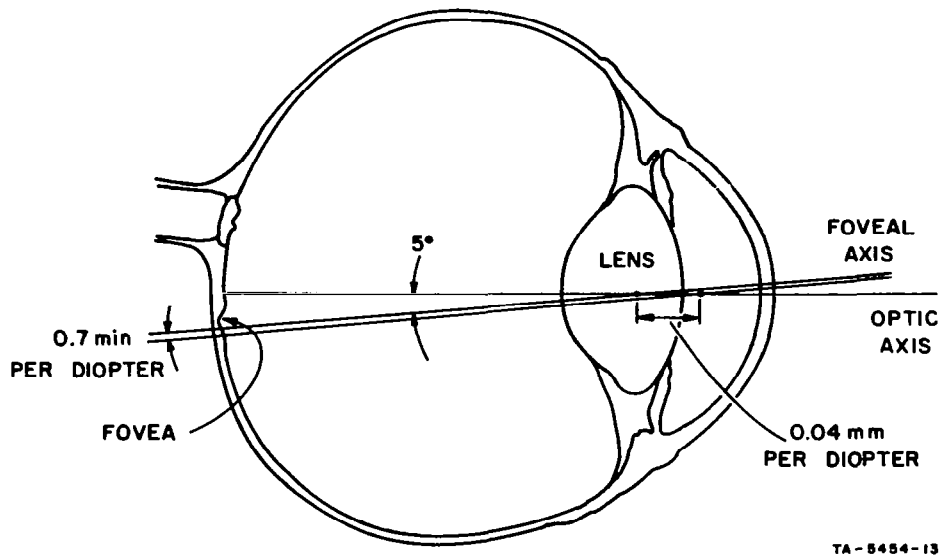


FIG. VII-3 LATERAL SHIFT OF IMAGE POSITION CAUSED BY AXIAL SHIFT IN EQUIVALENT LENS POSITION WITH CHANGE IN ACCOMMODATION

Experiment: Edge Polarity. This lateral shift on the retina is of course independent of the polarity of an edge, i.e. whether white to the left or white to the right. Thus, for one polarity of edge, this shift adds to the shift due to lateral inhibition (in Fig. VII-2), and for the opposite polarity it subtracts. Although the shift due to optics is on the order of only a tenth that due to lateral inhibition, the net difference in movements is nevertheless 20 percent; i.e. proportional to 1.1 units and 0.9 units. This may be sufficient to yield a measurable difference in accommodation response to edges of opposite polarity.

Note on Stabilized Images: We should note that a few-tenths diopter lens vibration results in a lateral vibration of the retinal pattern of about $0.2'$ of arc. Results from stabilized image experiments show that such a vibration amplitude can seriously affect the disappearance and fading of images normally associated with well-stabilized images. Ratliff (1965, p. 175), for example, shows a plot of the effect of various amplitudes and frequencies of superimposed movements on the disappearance of images. It may well be that for good stabilization of an image the effects of lens vibration must also be nullified.

D. Error in Initial Direction of Response

Consider an in-focus edge *A* positioned as in Fig. VII-4. An abrupt change in focus will blur the edge according to curve *B* so that the peak of the processed curve falls outside the receptor field. In this case, small "test" changes in accommodation—whether due to vibration or hunting—could increase the defocus to position *C* and lead to erroneous outputs.

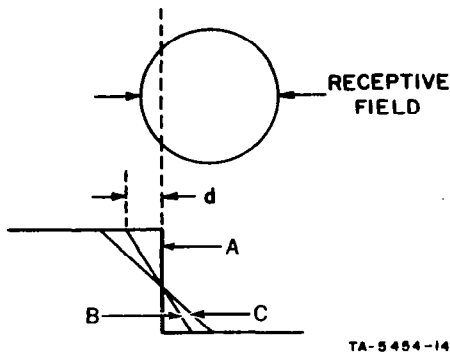


FIG. VII-4 POTENTIAL AMBIGUITY CAUSED BY AN ABRUPT FOCUS CHANGE. Abrupt focus change moves input pattern too near or beyond edge of receptor field.

The initial position of the in-focus edge varies considerably with small fixation movements (microsaccads). For a given distribution of saccad movements, or of initial positions of the in-focus edge, we could estimate the expected percentage of initial errors as a function of the shift distance d , assuming that a final position of the blurred edge too near the edge of the field, or outside of it, leads to ambiguity. The larger d , the larger the expected percentage of errors. We would also expect different results for different image patterns.

Troelstra, et al. (1964) report a large number of incorrect initial responses to 2 diopter step changes in focus, Fig. VII-5. Every false start is corrected, however, so that final accommodation is always correct. They do not state the condition of the pupil in these experiments; but if we assume a 5 mm pupil, the corner shift d in Fig. VII-4, for a 2 diopter change, is about $15'$ of arc. If we indeed have ambiguity near the edge of the field, we might well expect a relatively large number of initial errors for this magnitude of abrupt defocus, at least for initial placement of the edge (i.e. curve *A*) near the left edge of the field. For an initial placement of the edge near the right, we would expect a small probability of error.

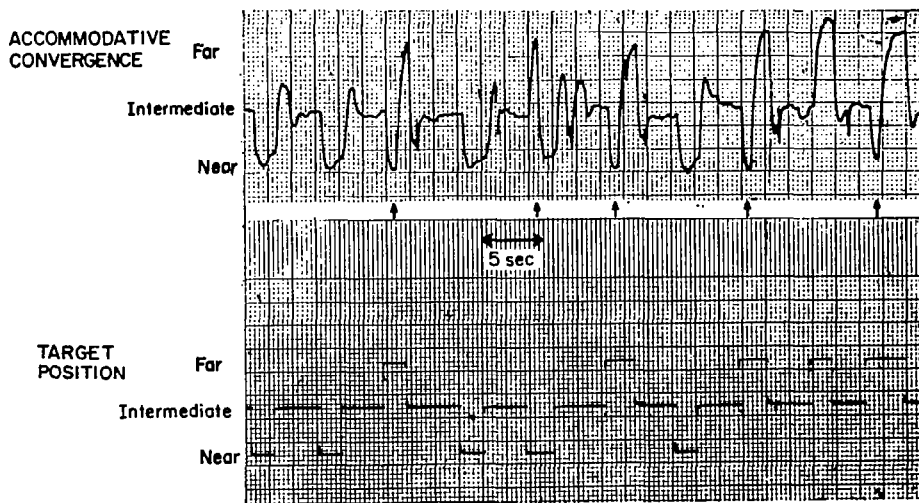


FIG. VII-5 TEN RESPONSES WITH FIVE INITIAL ERRORS OF RESPONSE

Source: Troelstra et al. (1964)

Experiment: Dependence on Initial Eye Position In view of this discussion, it would seem very important to be able to monitor eye position simultaneously with accommodation experiments to determine any correlation, as predicted here, between eye position at the moment of an induced defocus, and the probability of initial error in response.

E. Ring Model

The first "layer" of lateral inhibition processing represents rather local, point-function processing. In a next "layer" of processing we must somehow monitor the whole set of outputs from the first field. For this next "layer" we could visualize a total summation of outputs of all cells of the first layer. With a relatively large threshold in each input connection of the second "layer," we would obtain rather large changes in output with small changes in focus.

With a simple summation over the field, however, lateral movements of the edge as described above could cause ambiguity. For any shape of receptive field there exists some orientation for which lateral movement of an edge would change the total length of intercept over the receptive region, as suggested in Fig. VII-6(a) for a circular field. To obtain a truer measure of peak magnitude in the field it would therefore be necessary to normalize the output, i.e. divide the output by some measure of the total length of intercept. In the case of the lens vibrations, the lateral shift is perhaps only several minutes of arc, which represents a relatively small movement over a 30' receptive area. With a fairly well-centered edge pattern, this magnitude of lateral shift would probably not lead to ambiguity—though near the edge of the field even a few minutes shift could lead to a significant change in length of intercept, and hence possible ambiguity in output. This could well be one of the factors involved in errors in initial direction of response discussed in the last section.

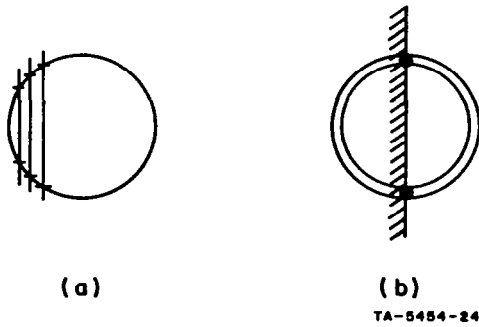


FIG. VII-6 EFFECT OF LATERAL MOVEMENT ON INTERCEPT OF EDGE ACROSS RECEPTOR FIELD
 (a) Disk model
 (b) Ring model

We could partially circumvent ambiguity from this cause by hypothesizing an annular receptive region around the periphery of the receptive field, as suggested in Fig. VII-6(b). In this case an edge would result in two bright "spots" on the annulus rather than a bright line across the entire region. Lateral movement would result only in a shift of the spots with relatively small change in integrated output.

In view of the very sparse experimental data available at this time, we cannot propose taking such a ring model too seriously. Nevertheless, it is interesting to recall one of Fincham's results (1951). Using subjects who could fixate "very well," he found that with fixation on a small disk object of a few minutes diameter, there was no accommodation tracking. Only when a subject was permitted to make an eye movement, estimated at greater than 6' of arc, would the automatic focus control react. Such a result is at least consistent with a ring model having an insensitive central region.

VIII CHROMATIC ABERRATION IN ACCOMMODATION CONTROL

A. Multiple Receptive Fields

We argued previously that a multiple receptor system that simultaneously samples different planes of image space could be useful in focus control. The visual color system offers possibilities of this nature. Although the three receptor systems are physically in the same retinal plane, they in effect sample different image planes because of the effects of chromatic aberration (i.e. the variation in focal length with the wavelength of illumination.) Let us try to determine whether our model can reasonably be expanded to include chromatic effects.

Campbell (1957) notes as much as 2 diopters shift in refractive strength from one end of the visual spectrum to the other, as shown in Fig. VIII-1. Figure VIII-2 represents the visual action spectra of the three classes of human retinal receptors. With broad-band "white" illumination, each color field is sensitive to all of the differentially focused images over its corresponding spectral band. For simplicity, however, let us simply assume that the total 2 diopter aberration is divided so that there is an average of one diopter shift from red to green, and 1 diopter shift from green to blue.

Using the notation for a ring model (although a uniform disk would do as well) let us assume now, as a simple extension of the accommodation control model, that there are three coincident rings, one for each color field.

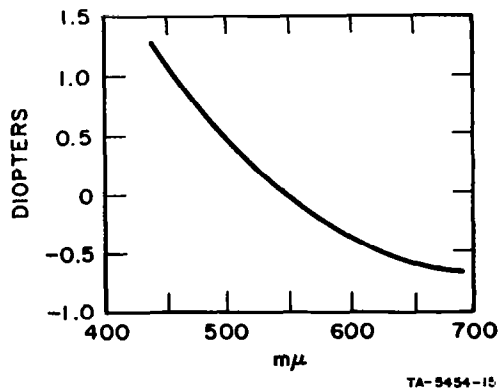


FIG. VIII-1 DIFFERENCE IN FOCUS
AS A FUNCTION OF
WAVELENGTH OF
ILLUMINATION
Source: Campbell (1957)

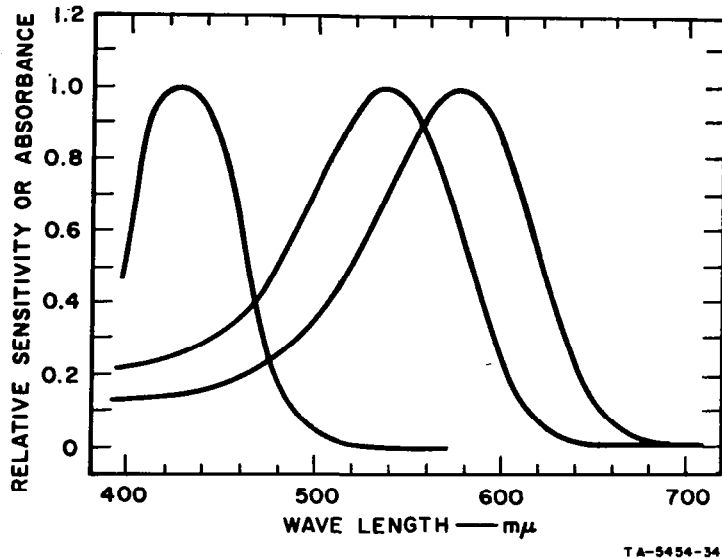


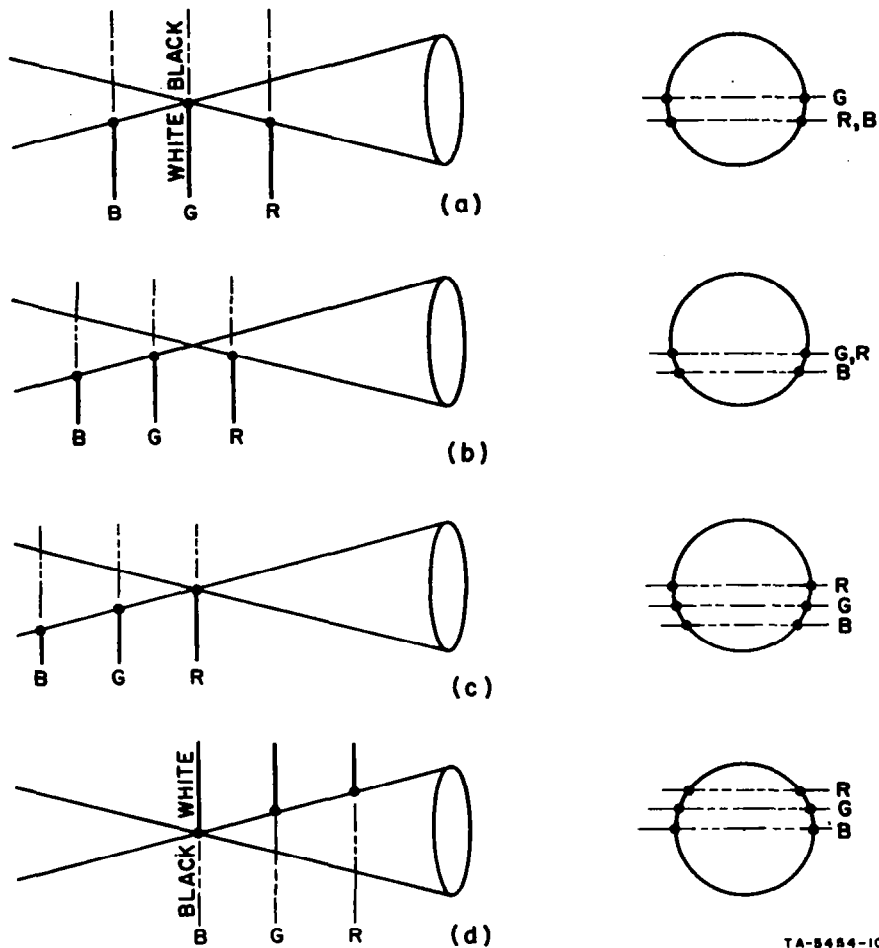
FIG. VIII-2 ACTION SPECTRA OF COLOR PIGMENTS

Corrected for distortions caused by ocular and macular distortions. λ_{max} of the blue-, green-, and red-sensitive pigments appear at about 430, 540, and 575 $m\mu$. All curves have been given the same arbitrary height for comparison. Source: Wald (1965)

Consider a black-white edge pattern. With the dioptric system set for focus in the green, the red and blue versions are then nominally one diopter out of focus. This condition is illustrated in Fig. VIII-3(a) by imagining the three receptor planes as being physically separated from each other by 1 diopter. In this case the pair of bright spots on the red and blue rings would be coincident and displaced from the pair of spots on the green ring. The reason for this displacement, as discussed earlier, is that with neural-unit processing the bright spots tend to track the bright corner of the image pattern. Under our present assumptions the red and blue images are equally blurred and thus would have the same magnitude of lateral shift in their bright spots.

For the cases presented earlier in the report, the exact lateral position of a bright edge on the receptive field was not too important, unless the edge fell too near or beyond the edge of the receptive field (Sec. VII-D) or if it affected the measure of the peak amplitude (Sec. VII-E). However, a measure of the differential shifts in a set of overlapping fields offers additional possibilities. This is particularly interesting in the case of multiple color fields, since the relative position of the bright spots depends on the geometry of the imaging and not on the relative intensities of the color components (except insofar as the intensity of an input pattern affects the fine structure of the neural-unit processing). Hence, any technique of accommodation control based on a measure of positional differences in the three fields will not be affected by moderate changes in the intensity of the chromatic components.

Fig. VIII-3(b) shows the effect of a shift in focus toward the red. With a nominal $\frac{1}{2}$ diopter shift in focus, the red and green pictures are now equally out of focus. In this case the red



TA-5484-10

FIG. VIII-3 SEPARATION OF COLOR FIELDS DUE TO CHROMATIC ABERRATION

- (a) Focus on green image
- (b) 1/2 diopter over-accommodated
- (c) 1 diopter over-accommodated
- (d) 1 diopter under-accommodated with reversed edge polarity

and green spots would be superimposed, and displaced from the blue spots. With another 1/2 diopter displacement, the red image would be in focus and the pairs of bright spots would appear in the order *R, G, B*, as in Fig. VIII-3(c).

B. Control Algorithms; Range of Control

If these relative displacements of the peaks in the color layers are actually important in focus measure, then we are faced with defining a control algorithm; i.e., a method by which these shifts are measured and utilized. The most we can do at the moment, however, in view of the sparse data available, is to make some observations regarding the possibilities.

Red-Blue Control. We must consider control algorithms for both polarity and magnitude of defocus. Let us first consider just the red-blue separation. For our purposes here, let us assume

that focus on the green, as in Fig. VIII-3(a), represents optimum focus. In optimum focus, then, the red-blue separation is zero. With increased defocus, we see from Fig. VIII-3 that the red-blue difference grows monotonically. Beyond 1 diopter defocus, however, the difference remains constant. For opposite polarity of defocus the difference is of the opposite polarity. We might therefore think that the red-blue shift alone would yield polarity as well as magnitude information. However, the polarity control from red-blue shift alone would be ambiguous, since we would obtain the same red-blue separation of defocus if the edge were reversed.

Unambiguous control could be obtained, however, from a measure of red-blue shift, together with a mechanism to determine edge polarity (i.e. whether it is bright on the left or the right side of the edge). Polarity control would be correct over a wide range, though the amplitude measure would saturate, as noted above, at the magnitude of chromatic aberration, namely about ± 1 diopter.

Red-Green-Blue Control. Unambiguous polarity control can also be obtained from comparative displacements on all three fields, without the need for separate monitoring of edge polarity. From Fig. VIII-3(b) we see that if the red-green separation is less than the blue-green separation we must decrease accommodation. The opposite condition implies under-accommodation and a need to increase accommodation. Hence, we can consider the following algorithm for polarity control:

$$\begin{aligned} |R-G| > |B-G| &\rightarrow \text{increase accommodation} \\ |R-G| < |B-G| &\rightarrow \text{decrease accommodation} \end{aligned}$$

where $|R-G|$ is a measure of the physical separation of the red and green edges, and $|B-G|$ is a measure of the blue-green separation.

This algorithm is useful, however, only up to a magnitude of defocus represented in Fig. VIII-3(c), i.e., about 1 diopter. Beyond that magnitude of defocus $|R-G| = |B-G|$. Ambiguity at this level of defocus also arises because the same alignment of spots in Fig. VII-3(c) is obtained by a 1 diopter defocus of the opposite polarity and an opposite polarity edge, as illustrated in Fig. VIII-3(d). Hence, the algorithm can yield unambiguous polarity control up to ± 1 diopter or so. Amplitude control could again be obtained from a measure of $|R-B|$ shift. At the present time, there is no available data on the range of chromatic control. To test, in any case, whether such physical shifts as are discussed here might actually be involved in chromatic focus control, we can attempt to generate conditions in which the normal relative positions are altered. Let us consider one such possibility.

Experiment: Shifted Color Pattern. Consider an edge-pattern in which the blue and red components are slightly shifted relative to the green component. The magnitude of shift in the object pattern is adjusted so that all bright spots on the retinal rings are superimposed when the image is focused on green. (Recall that the relevant magnitude of shift depends on pupil size, being about 7.5' for 1 diopter defocus and a 4.5 mm pupil.) Tracing rays in this configuration, we find that with any magnitude of defocus toward the blue (i.e., under-accommodation) the red and green spots remain superimposed. (Similarly, for any defocus toward the red, the blue and green dots remain superimposed). But with a normal pattern, superimposed red and green spots call for decrease in accommodation, i.e., toward the blue. If control based on relative displacement is valid, then we might suspect that with subjects who rely on chromatic information for accommodation control,

there might be a tendency toward accommodation instability with this pattern; an initial defocus toward blue seems to call for even greater defocus toward blue, and an initial defocus toward red seems to call for even greater defocus toward red.

C. Monochromatic Light

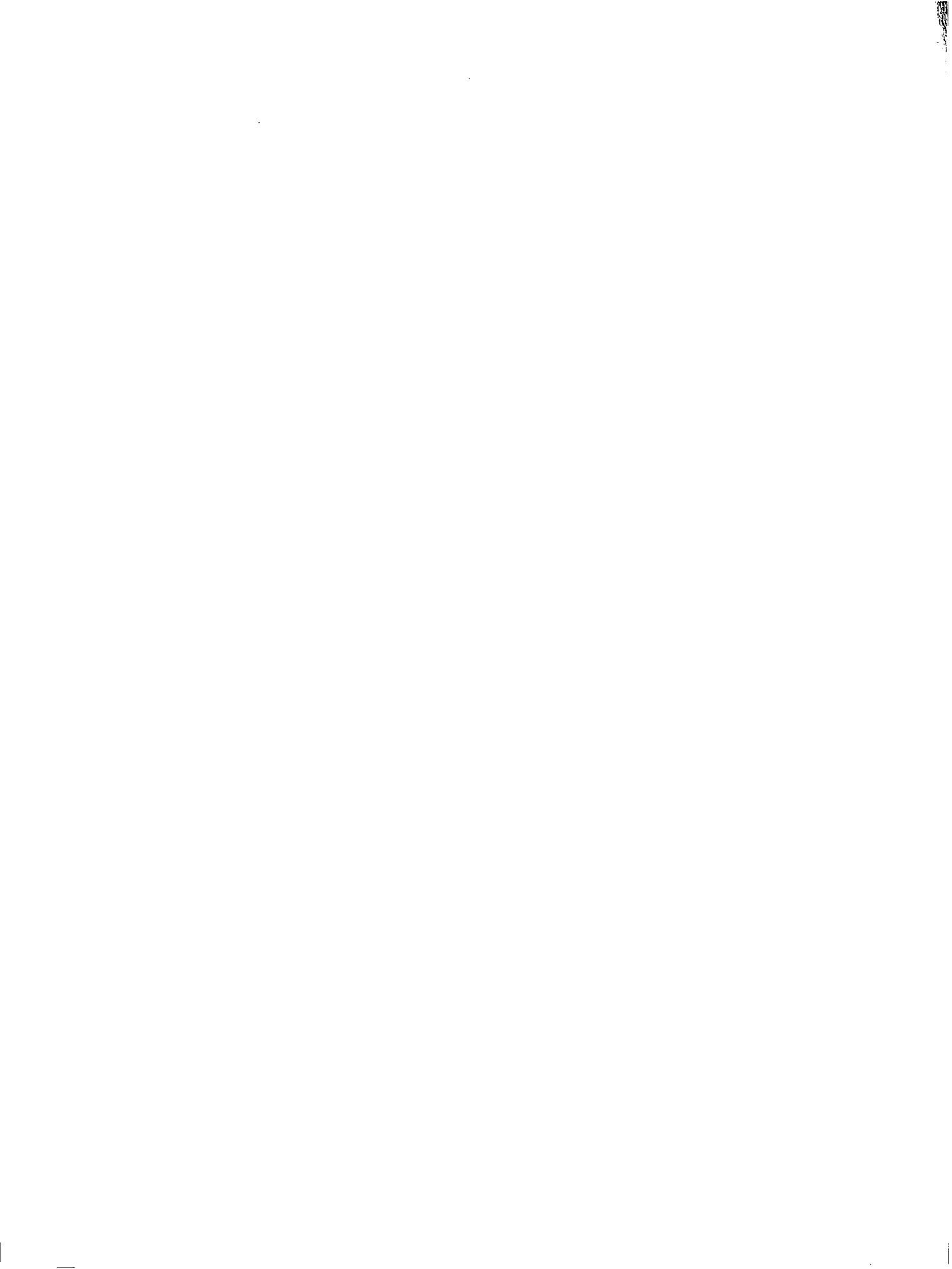
Recall that with monochromatic yellow light Fincham (1951) found that his subjects divided into three large groups. One group responded as well in accommodation reaction with monochromatic light as with white light. We might assume here that these subjects had a well developed system based on movement. Another group had no response whatever, although they were conscious of blur. We might equally well assume that these subjects had not developed accommodation control based on movement, but relied on chromatic aberration. A third group showed the same polarity of accommodation response with the insertion of a positive lens as with insertion of a negative lens.

With monochromatic light, exactly the same pattern would show on all three color fields. In the case of a yellow monochromatic light the red and green pictures would be about equally strong, but the blue picture would be very weak. We might possibly assume that the third group of subjects ordinarily has mixed control, based on movement and color, and that in this case the movement system signals a need for focus correction, but the fact of equal red and green pictures, and a very weak blue picture, yields incorrect control information. If we assume that the blue picture is essentially absent, then the $|R - B|$ measure would be ambiguous in the first model, and the $|G - B|$ measure would be ambiguous in the second model.

There is so little data available on chromatic effects that further speculation at this point would be fruitless. It seems rather clear, however, that a number of experiments in monochromatic light would be quite useful.

Experiments: Monochromatic Illumination. It would be most interesting to know whether with a blue-green monochromatic light the same three groups would form in Fincham's experiment; and in particular whether the third group would show a decrease in accommodation for defocus of either polarity, on the basis of equal green and blue images and a very weak red picture.

A number of possible experiments based on the use of multiple monochromatic sources are also immediately apparent: in particular, various combinations of two and three monochromatic sources. Consider, for example, a white illumination source composed of red, green, and blue monochromatic beams. Based on any measure of spatial separation, as discussed above, we could expect differences in accommodation reaction with shifts in the wavelengths of these monochromatic sources. For example, for a given edge configuration and magnitude of defocus, the magnitude of the $R-G$ measure would change with changes in wavelength of the red or green illumination sources.



IX PROGRAMMING THE RESPONSE

A. Recapitulation

An overall model for automatic focus control must consider: (1) what portion of the retina is functionally involved in focus control; (2) what kind of processing is performed on that portion of the retinal image to determine the state of focus; and (3) how the response is programmed.

As to (1), we argued for a small central zone of the retina to be functional in focus control, actually a sub-portion of the central fovea perhaps 30' wide. With regard to image processing, we showed in Sec. V how a measure involving the total magnitude of spatial derivative over the field can explain certain gross accommodation data, though not fine-focus control. For fine-focus control we developed a model in Sec. VII based on a measure of the peak value of spatial derivative over the field. In Sec. VIII we showed how a triplet of such fields, one for each color, could explain certain chromatic effects. In this section, we consider how the processed output signals—the measure of defocus—might be used in control of the ciliary muscles.

B. Dynamic Response

Typical monocular dynamic responses taken from Campbell and Westheimer were shown in Fig. III-3. In Fig. III-3(a) the stimulus was a 2 diopter change from zero accommodation, and subsequent return. Campbell and Westheimer noted that

“The maximum velocity reached during a 2D movement is of the order of 10D/sec. There is an increase in the maximum velocity with increase in the extent of movement, but we have not yet studied this relationship systematically since we find it difficult to record single-sweep accommodation responses exceeding 3D, other than voluntary ones.”

They further noted (p. 294) that

“The form of the single-sweep accommodation responses is to a first approximation exponential with an average time constant of about 0.25 sec. . . .”

In connection with Fig. III-3(b) the authors note increased variability in the response if there is a change in target blur but not in image size. Figure III-3(c) shows responses to various width pulses of object distance. Note that the duration of the response almost exactly matches the duration of stimulus change, and that because of the long reaction time the response for short stimulus pulses can actually begin after the stimulus has returned to its initial condition. The authors note that for pulses as short as 100 msec the responses are small or even completely absent.

C. Fixation Saccads

When we think of locating an object in space, we tend naturally to think in terms of both its distance and its angular position. The latter is generally referred to as “fixation” of the object, and the former as “accommodation.” Because the eye-movement system is subject to muscle drifts and tremors, it is not unexpected that fixation actually involves a continual series of correction movements (microsaccads). It is necessary to investigate how these saccadic movements might affect accommodation control.

Since we would like both to fixate an object and to focus on it at the high-resolution portion of the retina, it would not be surprising to find that both the fixation and the accommodation control systems operate from the same basic set of retinal receptors. We might, in fact, ask whether the model for accommodation, or some extension of it, might not also be useful in eye-movement control. For example, consider a sharply imaged point falling within the confines of a retinal ring. Because of eye movements the spot will eventually cross the ring. From the position of the crossing, suitable control signals could be generated for the next correction saccad. Young (1965) discusses a model of this type to explain the variation in saccad response time with the amplitude of the saccad.

Experiment: Focus-Fixation Interaction. In any case, an experiment to determine whether neural-unit processing is involved in eye-movement control would involve measuring any shift in the average eye-fixation position with differing amounts of image defocus. Recall that neural-unit processing leads to a significant lateral shift of the peak with defocus—e.g. a 7.5' shift for a 4.5 mm pupil and one diopter defocus in Fig. VI-4(b). The question here really is, what part of a blurred edge does the fixation system operate on? Our model would lead us to speculate that it mainly tracks the bright corner position.

D. Intermittent Control Model

An important question involved in accommodation control is whether the state of focus is continuously monitored, or if there is any kind of sampling or intermittent operation. Whether or not the accommodation system actually operates according to the processing model developed earlier, it seems clear that some sort of relatively complex spatial-temporal two-dimensional processing is performed. If we consider the gross changes to be expected—e.g. in a spatial derivative pattern—as a result of an abrupt change in focus, or an abrupt microsaccad, it is difficult to conceive of a continuous mode of operation without significant periods of “incorrect” output. It is tempting therefore to consider a control model in which there is at least some period for transients to “settle” after any substantial change in the input pattern.

Having proposed such a mode of operation, we must next ask what initiates this “settling” period. In the case of an eye movement, it may be either the eye movement itself or the resulting change of pattern on the receptor sheet. If it is the latter, then we would suspect that a lateral movement of the target might also initiate a similar response cycle. If the cycle is initiated by the eye movement itself, then we must ask whether any other effects can also initiate a timing cycle.

Another important question is whether the correction process itself is a continuous closed-loop process, or consists of open-loop ballistic movements. Recall the comment of Campbell and Westheimer (1960, p. 294) that the form of the single-sweep response is to a first approximation exponential, with an average time constant of 0.25 sec. We could reasonably expect an exponential response from a step change applied to a damped muscle system, or from a closed-loop system in which the “error” signal smoothly decreases as focus smoothly improves. Certain experimental results tend to make us favor the ballistic open-loop response. According to Fig. III-3(c), we see that a full-term response to a short pulse stimulus can actually begin after the stimulus has ended. We would tend to describe the process in terms of an abrupt pattern change initiating

a "processing epoch" consisting of a delay, a measure of defocus, and then a ballistic response. A second abrupt pattern change (the end of the stimulus) initiates a second cycle that follows the same course.

The results in Fig III-3(d), regarding accommodation tracking of a slowly changing defocus, are also quite interesting. Note that although the target is tracked in a general overall sense, there are occasional vast excursions in accommodation. The target velocity in this experiment (in diopters per second) is quite small, so that if the target movement system was not jerky, we would probably not expect "processing epochs" to be initiated by the target movement itself, but perhaps only by eye movements. It would be very interesting to see a simultaneous record of fixation eye movements during the response interval. We might guess that some or all of the small submovements in accommodation are temporally related to fixation movements, each one initiating a new processing epoch, or interval. It would be especially interesting to see if the large incorrect excursions correspond with particularly large saccads which drive the fixation point too close to or beyond the edge of the receptive field, as discussed in Sec. VII-D.

Another important point regarding a ballistic output model is that even when the initial polarity of the response is wrong the response appears to have basically the same duration and exponential shape as a correct response. (See Fig. VII-5.) This is hard to explain with a closed-loop model.

Classifying Pattern Changes. Pursuing the notion that a sufficiently large change in retinal pattern initiates a ballistic correction movement, we can next consider what types of movements might initiate response cycles. For example, an average-size involuntary saccad of 10' would sweep an image a third of the way across a 30' receptive region, and we would be inclined to assume that such a movement could initiate an accommodation cycle. On the other hand a small saccad, or a saccad parallel to a contrast edge, would result in a relatively small change in the retinal image and might not therefore initiate such a cycle.

Changes in target location result in three simultaneous effects: change in focus, change in subsequent image size, and lateral shifts. With object movement along the visual axis there will nominally be no lateral shifts in the image; thus relatively small target shifts along the visual axis might not initiate a timing cycle. There can be large effects for target shifts off the optic axis, however, which might according to our hypothesis initiate timing cycles. With too large a lateral shift, there would in fact have to be a saccadic eye movement to return the point of interest to the relatively small processing region.

To appreciate the potential magnitude of lateral shift with target motion, consider fixated target A in Fig. IX-1, which is a distance d_1 from the eye. Let the target shift abruptly to a new position A'' which is a distance d_2 from the eye, along an axis displaced by an angle α from the visual axis. A rough approximation to the angular displacement β of the image, for a given angular shift α is

$$\beta = \left(\frac{d_2 - d_1}{d_2} \right) \alpha \quad (\text{IX-1})$$

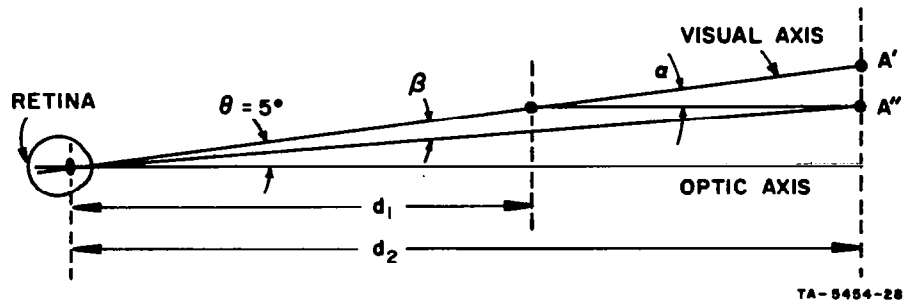


FIG. IX-1 RELATIONSHIP BETWEEN CHANGE IN VISUAL ANGLE AND CHANGE IN TARGET POSITION
Change in visual angle β for a lateral shift α accompanying a change in target distance from d_1 to d_2

For a given value of α , the lateral shift β (per diopter change in target distance) increases with the initial distance d_1 . For example, a change from 4 to 3 diopters corresponds to a shift

$$\beta = \left(\frac{1/3 - 1/4}{1/3} \right) \alpha = \left(\frac{4-3}{4} \right) \alpha = 1/4 \alpha \quad (\text{IX-2})$$

whereas from 1 to 0 diopters, $d_2 = \infty$, so that the ratio is unity. Thus, relatively large image shifts can occur even for relatively small values of α . We see then the need for rather precise control of target displays for experiments in which there is any attempt to maintain target movement along the visual axis.

The following experiments might help evaluate the feasibility of an intermittent accommodation-control model and the interaction of accommodation control with eye movements.

Experiment: Reaction Time for Different Target Movements. To test some of these classification arguments we could measure accommodation reaction time to target movement between two fixed distances, say d_1 and d_2 , but with varying magnitude of lateral shift α . An important result would be finding substantially different reaction times for large and small magnitudes of α . On the basis of an intermittent model, with cycles triggered only by abrupt pattern shifts, we would expect smaller reaction times for large α (large enough, that is, to initiate an accommodation cycle but perhaps not an eye-movement). For a small α movement that does not initiate a cycle, response would have to wait until a subsequent cycle, triggered perhaps by an eye movement.

Experiment: Timing of Object Movement to Saccadic Movement. If we assume that a saccad can initiate a timing cycle, then accommodation reaction time should depend also on just when a target movement is made with respect to the last, or in fact, the next saccad. A series of experiments involving varying timing relations to adjacent saccad intervals would therefore help in evaluating any ideas regarding intermittent control models.

Experiment: Laterally Moving Objects. We might also ask about accommodation to an object swinging laterally at a fixed distance. Under conditions of movement such that there was relatively smooth pursuit eye-tracking, it would be possible to have a reasonably stable image, at

least during some intervals, and we might therefore expect reasonably steady accommodation response. However, for movements outside the smooth pursuit range, and with an unfamiliar object configuration, we might get relatively large transient changes in accommodation even at a constant distance from the eye.

E. Hypothesis: Lens Vibrations as "Accommodation Saccads"

We tend to think of involuntary eye-movement saccads as being correcting movements for the various sorts of drifts and tremors that naturally occur in a living muscle system. We can logically argue the need for similar correcting movements in other control systems such as the lens. As with fixation saccads, there might indeed be a similar mechanism in accommodation control so that when the accommodation error becomes too large there is an "accommodation saccad," though we have no clear evidence at the moment that this is the case. Let us continue then simply on the assumption that a sufficiently large pattern change on the retina initiates an accommodation correction cycle; in particular, a change resulting from an eye-movement or a target movement.

The eye-movement system has very fast response; eye-movement records typically have the appearance of abrupt transitions superimposed on slower drift components. With similar stimuli, but a much slower responding system, the record would have more the appearance of a series of positive and negative exponential waveforms superimposed on a corresponding slow drift. Recall again Campbell and Westheimer's observation that single step accommodation responses are typically exponential with a time constant of about 0.25 sec. If correction cycles were initiated every 0.25 sec. there would be a continual series of alternating positive and negative exponentials which could readily be interpreted as a "hunting" movement or "oscillation" at a 2 cps rate.

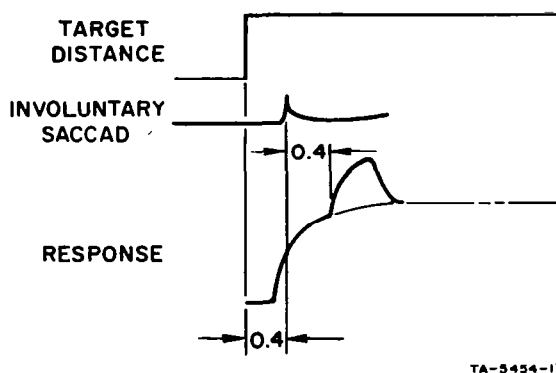
Of course, involuntary saccads do not occur at a uniform rate but have a distribution over a wide range of time intervals. An interval-histogram for fixation saccads would be small for both very small intersaccad intervals and for very large intervals. Such histograms are not conveniently available and so it is not clear at the moment over what range of intervals the distribution actually peaks. (Preliminary examination of some of Cornsweet's fixation eye-movement records shows large numbers of occurrences in the 100-500 msec interval.) Some frequency response plots for eye tracking—e.g. Young and Stark (1963, p. 43)—show a peak in response at about 2.5 cps, which "reflects the large amount of energy in the eye response spectrum resulting from discrete eye movements at approximately 0.2 sec. intervals during eye tracking." It is readily conceivable then that the peak at about 2 cps in the spectral density plots obtained from continuous optometer records could be explained on the basis of accommodation correction cycles paced by involuntary saccads.

We can see, in fact, that such a hypothesis squares well with the experimental observation that the amplitude of the "oscillations" becomes very small in the presence of a small artificial pupil. If the oscillations are simply a series of correction movements, then we would naturally expect the amplitude to be small under conditions where the accommodation error is likely to be small, such as with a small pupil, and therefore a large depth of field.

The oscillation amplitude is also found to increase monotonically with accommodation level. Here we might argue that relaxed accommodation is the more natural rest state of the system, since with uniform white and dark fields accommodation relaxes to near infinity (though not quite—for an interesting discussion of the effects of an empty visual field on accommodation le-

vel see Whiteside, 1957). If we consider the relaxed position as the zero position, then for a given percent error in accommodation control the absolute error would be larger the greater the accommodation level, and so would the resulting accommodation corrections.

This model could predict the compound overshoots in response sometimes seen in accommodation records. Assume in Fig. IX-2 that an abrupt target movement initiates a correction cycle so that one reaction time, or about 0.4 sec later, the accommodation response begins. Since the target change is unsynchronized with eye movements, an eye movement can occur at any instant during the process (in fact, a target change might increase the probability of an eye movement occurring). Suppose that an involuntary saccad occurs a few tenths of a second after the accommodation correction begins. At this instant there is still a significant error in accommodation.



TA-5454-17

FIG. IX-2 COMPOUND RESPONSE WITH OVERSHOOT DUE TO EYE MOVEMENT OCCURING SOON AFTER TARGET MOVEMENT

If we assume that the eye movement initiates a new correction cycle, and that the reaction time is the same for the second cycle, then about 0.4 sec after the eye movement there will be a second exponential response added to the first response. This will result in an overshoot that will have to be corrected in a subsequent cycle. In Troelstra's records, Fig. VII-5 we see just such overshoots composed of double exponentials.

Experiment: Effect of Edge Orientation. Fixation saccads are not isotropic but occur more often in certain preferred directions (Nachmias, 1959), typically at 45° to the vertical. On the basis of our model, we might therefore predict different accommodation response to edges oriented parallel to and orthogonal to this direction, because saccads in the direction of the edge would not alter the retinal picture and therefore would not initiate accommodation correction cycles (according to our hypothesis). We might then find larger amplitude and perhaps lower frequency of "vibrations" for edges oriented along the preferred direction of involuntary saccads because of the less frequent correction cycles. On the basis of such a result, we might also predict differences in acuity along orthogonal axes.

X SUMMARY

This study has attempted to model the human visual accommodation system, starting directly with the retinal image. The models that are developed are reasonably consistent with existing data and offer a certain degree of understanding of the data. They are clearly tentative, however, since available experimental data are not only sparse but nonhomogeneous because of the difference in approach and instrumentation of various experimenters, and as much because of the general lack of models to coherently guide the selection of experiments.

The modeling is in three stages. Starting at the retina we ask: (1) What portion of the retinal picture is involved in accommodation control; (2) How that portion of the picture is processed to derive a measure of defocus; and (3) How that signal is in turn used to control the ciliary muscles.

The first question is probed in Sec. I-C, and we conclude that the relevant portion of the retina is a central region of the fovea, having a diameter of some 30' of arc, or 6 mils—the diameter of a coarse human hair. The second question is discussed in Sections II through VIII. It is shown how circuits based on lateral inhibition in neural-unit processing can yield a measure of defocus that is consistent with experimental data over several orders of magnitude of object size and illumination. In Sec. VIII we show how interaction between three overlapping receptor regions could account for certain chromatic effects in accommodation control.

The third question is discussed in Sec. IX. We tentatively propose an intermittent control model in which accommodation correction cycles are initiated by relatively abrupt changes in the retinal pattern caused, for example, by involuntary eye-movement saccads or certain target movements. A case is argued for a control cycle involving a sampling of the accommodation error followed by a ballistic corrective movement.

In terms of this control model the elusive lens "vibrations" appear to be no more than normal accommodation correction cycles. For a stationary target, these correction cycles are triggered primarily by the saccadic eye movements. In this case, the 2 cps peak in accommodation spectral density plots (Fig. III-1) can be traced to a similarly large component in spectral density plots for involuntary eye movements. On this basis it is clear why the "vibrations" become small with a small artificial pupil inserted in front of a dilated pupil: the depth of field is large, and the necessary corrections therefore small. The model also leads to an argument for the amplitude increasing monotonically with increased level of accommodation. Certain accommodation overshoots are also given a reasonable basis with this model, especially overshoots composed of compound exponential curves.

The potential role of these lens vibrations is still not clear. If in fact they turn out to be no more than "normal accommodation correction cycles" then it seems that we can fairly well write them off as far as accommodation measurement is concerned.

The models predict significant interaction between accommodation and eye-movements. One can logically argue for both systems sharing the same receptive region of the retina and even certain common processing features. Experiments are proposed which would help elucidate the nature of this interaction.

Although accommodation control appears at first as a relatively minor aspect of the general visual perception problem, we have seen that many of the same basic questions are involved in accommodation control as in general visual perception: the nature of the neural processing circuits; the effects of eye movements; the effects of chromatic content; and the possible intermittent sampling nature of the control. Understanding the nature of the accommodation system might therefore yield important insight and understanding concerning the general visual perception problem. In fact, the ability to accurately and continuously monitor accommodation and eye movements, binocularly, as well as monocularly, seems to provide a useful testing ground for many perceptual questions, regarding the effects of variation in the spatial, temporal, and chromatic content of the retinal images.

What is clearly needed to evaluate, alter, or expand the hypotheses developed here is a versatile experimental facility with which to perform a highly organized series of experiments; a facility involving at least accommodation monitoring, eye movement monitoring, and a visual display system that can be changed rapidly and synchronized with various aspects of accommodation and eye movement changes. We hope that subsequent experimental results and potential applications will justify our present enthusiasm for further study in this area.

REFERENCES AND BIBLIOGRAPHY

The bibliography is listed alphabetically by author. Items actually referenced in the text are indicated with an asterisk (*).

- *Abraham, S. V., "Accommodation in the Amblyopic Eye," *Am. J. Opth.* 52, pp. 197-200 (August 1961).
- Allen, M. J., "An Objective High Speed Photographic Technique for Simultaneously Recording Changes in Accommodation and Convergence," *Am. J. Opth.* 26, No. 7, pp. 279-280 (July 1949).
- Allen, M. J., "A Study Concerning the Accommodation and Convergence Relationship," AD 264937, *ASD Technical Report* 61-111 (May 1961).
- Allen, M. J., "Calibration of the Infrared Optometer," Technical Report AMRL-TDR-62-88, Life Support Systems Laboratory, Wright-Patterson Air Force Base (August 1962).
- *Alpern, M., "Accommodation," in *The Eye*, Vol. 3, edited by H. Davson, pp. 191-229 (Academic Press, New York and London, 1962).
- Alpern, M. and B. F. Larson, "Vergence and Accommodation," *Am. J. Opth.* 49, pp. 1140-1149 (May 1960).
- Armaly, M. F. and N. C. Jepson, "Accommodation and the Dynamics of the Steady State Intraocular Pressure," *Invest. Opth.* 1, No. 4, pp. 480-483 (August 1962).
- *Arnulf, A. and O. Dupuy, "Contribution a l'Etude des Microfluctuations d'Accommodation de l'Oeil," *Rev. Opt.* 39, No. 5, pp. 195-208 (May 1960).
- *Arnulf, A., O. Dupuy, and F. Flamant, "Les Microfluctuations d'Accommodation de l'Oeil," *Am. Oct. Oc.* 3, No. 5, pp. 109-118 (September 1955).
- Arnulf, A., O. Dupuy, and F. Flamant, "Les Microfluctuations de l'Oeil et Leur Influence sur l'Image Retinienne," *Optique Physiologique*, C.R. *Acad. Sci. (Paris)* 232, pp. 438-440 (January 1951).
- Ayrshire Study Circle, "An Investigation into Accommodation," *Brit. J. Physiol. Opt.* 21, pp. 31-35 (January-March 1964).
- Backer, W. D. and K. N. Ogle, "Pupillary Response to Fusional Eye Movements," *Am. J. Opth.* 58, pp. 743-756 (November 1964).
- *Bliss, J. C. and H. D. Crane, "Optical Detector for Objects Within an Adjustable Range," *J. Opt. Soc. Am.* 54, No. 10, pp. 1261-1266 (October 1964).
- *Bliss, J. C. and H. D. Crane, "Relative Motion and Nonlinear Photocells in Image Processing," in *Optical and Electro-Optical Information Processing* (M. I. T. Press, Boston, 1965).

- *Campbell, F. W., "Accommodation Reflex," *Brit. Orthoptic J.* 11, No. 13, pp. 13-17 (1954).
- *Campbell, F. W., "Correlation of Accommodation Between the Two Eyes," *J. Opt. Soc. Am.* 50, p. 738 (July 1960).
- *Campbell, F. W., "The Depth of Field of the Human Eye," *Opt. Acta* 4, No. 4, pp. 157-164 (December 1957).
- *Campbell, F. W., "The Minimum Quantity of Light Required to Elicit the Accommodation Reflex in Man," *J. Physiol.* 123, No. 2, pp. 357-366 (February 1954).
- Campbell, F. W. and A. H. Gregory, "Effect of Size of Pupil on Visual Acuity," *Nature* 187, No. 4763, pp. 1121-1123 (September 1960).
- *Campbell, F. W. and J. G. Robson, "High-Speed Infrared Optometer," *J. Opt. Soc. Am.* 49, No. 3, pp. 268-272 (March 1959).
- *Campbell, F. W. and J. G. Robson, "Moving Visual Images Produced by Regular Stationary Patterns," *Nature* 181, p. 362 (February 1958).
- *Campbell, F. W., J. G. Robson, and G. Westheimer, "Fluctuations of Accommodation Under Steady Viewing Conditions," *J. Physiol.* 145, pp. 579-594 (March 1959).
- Campbell, F. W., J. G. Robson, and G. Westheimer, "Significance of Fluctuations of Accommodation," *J. Opt. Soc. Am.* 48, No. 9, p. 669 (September 1958).
- *Campbell, F. W. and G. Westheimer, "Dynamics of Accommodation Responses of the Human Eye," *J. Physiol.* 151, No. 2, pp. 285-295 (May 1960).
- Campbell, F. W. and G. Westheimer, "Factors Influencing Accommodation Responses of the Human Eye," *J. Opt. Soc. Am.* 49, No. 6, pp. 568-571 (June 1959).
- *Campbell, F. W. and G. Westheimer, "Sensitivity of the Eye to Differences in Focus," *J. Physiol. (London)* 143, p. 18P (1958).
- Carter, J. H. Jr., "A Servoanalysis of the Human Accommodative Mechanism," *Arch. Soc. Am. Ophth. Optom.* 4, pp. 137-168 (O-P Book, University Microfilms, Inc., Ann Arbor, 1962).
- *Davson, H., editor, *The Eye*, 4 Vols. (Academic Press, New York and London, 1962).
- Elul, R., P. L. Marchiafava, and L. Nicotra, "Method for Measurement of Accommodation in the Cat," *J. Opt. Soc. Am.* 54, No. 3, pp. 380-386 (March 1964).
- *Fender, D. H., "Control Mechanisms of the Eye," *Sci. Am.* 211, No. 1, pp. 24-33 (July 1964).
- *Fincham, E. F., "Communications—The Accommodation Reflex and its Stimulus," *Brit. J. Ophth.* 35, No. 7, pp. 381-393 (July 1951).

- Fincham, E. F., *The Mechanism of Accommodation*, 8, *Brit. J. Ophth. Monograph Supplement VIII* (1937).
- Fleming, D. G. and J. L. Hall, "Autonomic Innervation of the Ciliary Body. A Modified Theory of Accommodation," *Am. J. Ophth.* 48, No. 3, Pt. 2, pp. 287-293 (September 1959).
- Fry, G. A., "The Effect of Homatropine Upon Accommodation-Convergence Relations," *Am. J. Optom.* 36, pp. 525-531 (October 1951).
- Fry, G. A., "Fundamental Variables in the Relationship Between Accommodation and Convergence," *Optom. Weekly* 55, pp. 21-26 (September 1964).
- *Haynes, H., B. L. White, and R. Held, "Visual Accommodation in Human Infants," *Science* 148, pp. 528-530 (April 1965).
- Hebbard, F. W., "Foveal Fixation Disparity Measurements and Their Use in Determining the Relationship Between Accommodative Convergence and Accommodation," *Am. J. Optom. and Arch. Am. Acad. Optom.* 37, No. 1, pp. 3-26 (January 1960).
- *Hess, E. H., "Attitude and Pupil Size," *Sci. Am.* 212; No. 2, pp. 46-54 (April 1965).
- Hill, R. V., "The Hyperbolas of Accommodation and Convergence," *A. M. A. Arch. Ophth.* 57, pp. 259-263 (February 1957).
- Itoi, M., N. Ito, and H. Kaneko, "Visco-Elastic Properties of the Lens," *Exp. Eye Res.* 4, pp. 168-173 (September 1965).
- Jampel, R. S., "Convergence, Divergence, Pupillary Reactions and Accommodation of the Eyes from Foradic Stimulation of the Macaque Brain," *J. Comp. Neurol.* 115, No. 3, pp. 371-397 (December 1960).
- Knoll, H. A., "The Relationship Between Accommodation and Convergence and the Elevation of the Plane of Regard," *Am J. Optom.* 39, pp. 130-134 (March 1962).
- Kramer, M. E., "Role of Suppression and Relative Accommodation in Orthoptic Prognosis," *Am. Orthopt. J.* 10, pp. 104-107 (1960).
- Luria, S. M., "Accommodation and Scotopic Visual Acuity," *J. Opt. Soc. Am.* 51, No. 2, pp. 214-219 (February 1961).
- *MACD., W., "The Electrophane Camera," *Electronics*, pp. 44-47 (March 1942).
- *Mackay, D. M., "Moving Visual Images Produced by Regular Stationary Patterns," *Nature* 181, pp. 362-363 (February 1958).
- Melton, C. E., "Neural Control of the Ciliary Muscle," Civil Aeromedical Research Institute, Oklahoma City, 63-5 (March 1963).
- Mizukawa, T. *et. al.*, "Studies on Accommodation. IV: The Resting Study of Accommodation," *J. Clin. Psych. (Tokyo)* 16, pp. 199-205 (February 1962).

- *Nachmias, J., "Two-Dimensional Motion of the Retinal Image During Monocular Fixation," *J. Opt. Soc. Am.* 49, No. 9, pp. 901-908 (September 1959).
- Ogle, K. N. and J. T. Schwartz, "Depth of Focus of the Human Eye," *J. Opt. Soc. Am.* 49, No. 3, pp. 273-280 (March 1959).
- *Ratliff, F., *Mach Bands* (Holden-Day, Inc., San Francisco, 1965).
- Ripps, H., G. M. Breinin, and J. L. Baum, "Accommodation in the Cat," *Trans. Am. Ophth. Soc.* 59, pp. 176-193 (1961).
- Ripps, H., N. B. Chirri, I. M. Siegel, and G. M. Breinin, "The Effect of Pupil Size in Accommodation, Convergence and the AC/A Ratio," *Invest. Ophth.* 1, No. 1, pp. 127-135 (February 1962).
- Ronchi, L. and G. Bottai, "Apparent Fine Structure of Defocussed Patches," report to the USAF under Grant N.AF-EOAR 63-4, Vol. 18, No. 4, pp. 533-547 (September-October 1963).
- *Southall, J. P. C., *Introduction to Physiological Optics* (Dover, New York, 1961).
- Stark, L., "The Dynamics of the Human Lens System," Quarterly Progress Report No. 66, Research Laboratory of Electronics, MIT, Cambridge, Mass., pp. 337-351 (July 1962).
- *Stark, L., "Neurological Servomechanisms: Section III, The Lens," Special Final Report, Bioengineering Section, College of Engineering, University of Illinois at Chicago (May 1965).
- Stark, L., "Pupil and Lens Control Systems," Progress Report No. 3, Contract No. NAS 2-2122, National Aeronautics and Space Administration, Ames Research Center, Moffett Field, California (April 1965).
- Stark, L. and Y. Takahashi, "Absence of Odd-Error Signal Mechanism in Human Accommodation," *Proc. IEEE Int. Conv.*, New York, pp. 202-214 (March 1965).
- Stark, L. and Y. Takahashi, "Accommodation Tracking," Quarterly Progress Report No. 67, Research Laboratory of Electronics, MIT, Cambridge, Mass., pp. 205-212 (October 1962).
- Travi, O. C. and C. E. Fernandez Mendez, "Carencia Congenita de Acomodacion," *Arch. Oftal. (Buenos Aires)* 36, pp. 165-166 (July 1961).
- *Troelstra, A., B. L. Zuber, D. Miller, and L. Stark, "Accommodative Tracking: A Trial and Error Function," *Vision Res.* 4, pp. 585-594 (June 1964).
- *Wald, G., "The Receptors of Human Color Vision," *Science* 145, pp. 1007-1017 (September 1964).
- Wallach, H. and C. M. Norris, "Accommodation as a Distance-Cue," *Am. J. Psychol.* 76, pp. 659-664 (December 1963).
- *Walls, G. L., *The Vertebrate Eye* (Hafner Publishing Co., New York, 1963).

- *Warshawsky, J., "The Focusing Servomechanism of the Human Eye," Ph.D. thesis, Northwestern University (June 1963).
- Warshawsky, J., "High-Resolution Optometer for the Continuous Measurement of Accommodation," *J. Opt. Soc. Am.* 54, No. 3, 375-379 (March 1964).
- Weber, G., "Study of the Relations Between Accommodation, Convergence, and Fusion," *Optik (Germ.)* 15, pp. 474-480 (August 1958).
- *Westheimer, G., "Accommodation Measurements in Empty Visual Fields," *J. Opt. Soc. Am.* 47, No. 8, pp. 714-718 (August 1957).
- Westheimer, G., "Amphetamine, Barbiturate, and Accommodation-Convergence," *Arch. Ophthalm.* 70, No. 6, pp. 830-836 (December 1963).
- *Westheimer, G., "Optical and Motor Factors in the Formation of the Retinal Image," *J. Opt. Soc. Am.* 58, No. 1, pp. 86-93 (January 1963).
- *Whiteside, T. C. D., *The Problems of Vision in Flight at High Altitude*, Appendix H, p. 153 (Butterworth's Scientific Publications, London, 1957).
- *Young, L. R., "Control Aspects of Human Saccadic Eye Movements," Progress Report No. 2 on Physiology of the Visual Control System, Contract NAS 2-1328 (February-May 1965).
- *Young, L. R. and L. Stark, "Variable Feedback Experiments Testing a Sampled Data Model for Eye Tracking Movements," *IEEE Trans. HFE-4:1*, pp. 38-51 (September 1963).
- Zajac, J. L., "Convergence, Accommodation and Visual Angle as Factors in Perception of Size and Distance," *Am. J. Psychol.* 73, pp. 142-146 (March 1960).

APPENDIX I

DETERMINING BLURRED-EDGE PROFILES

Consider a uniformly illuminated disk, which in focus subtends an image diameter D , as in Fig. AI-1. If the viewing screen is moved out of the image plane each point of the sharp image will blur to a circular disk—a blur disk—of diameter d . (The shape of the blur disk actually depends on the shape of the lens aperture. For our purposes here, assume a circular lens)

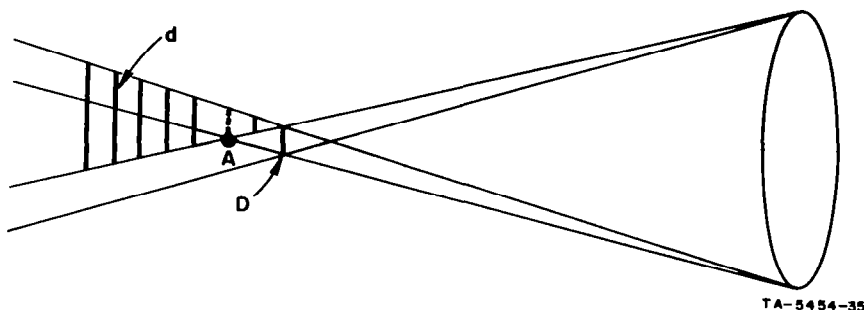
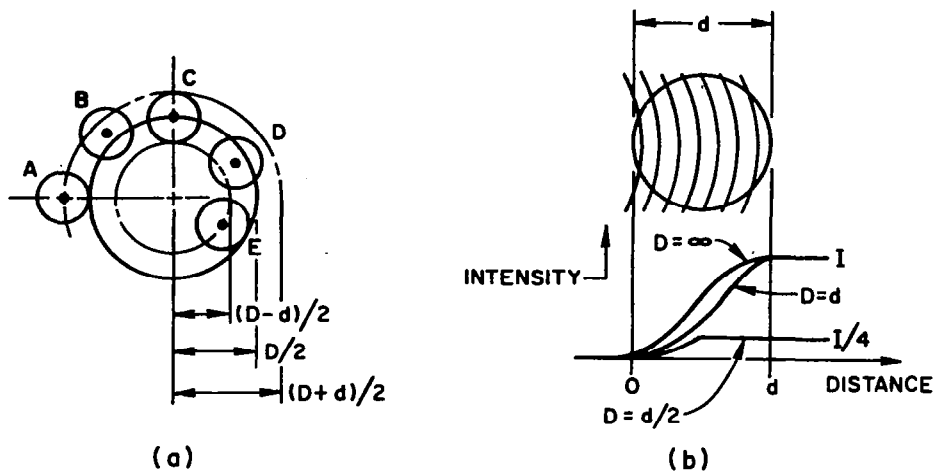


FIG. AI-1 GEOMETRY OF AN IN-FOCUS DISK IMAGE AND OF THE BLUR DISK OF AN OUT-OF-FOCUS POINT ON THE EDGE

shape. Assume also a uniform intensity over the blur disk, i.e. neglect diffraction effects.) The magnitude of the blur disk depends on the magnitude of defocus. We can calculate the light intensity over the total blurred image in terms of these overlapping blur disks, there being one such disk for each point of the original in-focus image.

Assume for the moment a small magnitude of defocus, so that $d < D$. It is clear that the extent of the blurred image will be $D+d$, the intensity becoming zero at that diameter. To calculate the intensity at any point of the edge it is necessary only to “count up”, so to speak, the number of points in the original in-focus image whose corresponding blur disks contribute light to the point in question. This results in the formation of a convolution integral the essence of which is to draw a blur disk about the point in question and to integrate over the area of the disk the total light in the in-focus image. To show the logic of this approach a few such disks are illustrated in Fig. AI-2(a). At points beyond radius $(D+d)/2$ there is no overlap whatever, or zero intensity. At radius $(D+d)/2$ the two disks just come in contact (position *A*). At progressively closer points the area of overlap monotonically increases. Position *C* corresponds to the edge of the original in-focus disk. As we reach radius $(D-d)/2$, namely position *E*, the overlap is complete and the intensity is maximum. The intensity is uniform from position *E* to the center of the original disk.



TA-5454-16

FIG. AI-2 GEOMETRY USED FOR CALCULATING EDGE PROFILE OF BLURRED DISK IMAGE

- (a) Overlay of blur disks on the disk image
 (b) Sweeping the image across a fixed blur disk

We see then that the defocused image has uniform intensity to a radius $(D-d)/2$, and has an edge width d . To find the intensity profile along the edge we can determine the light intensity for all overlap positions, as in Fig. AI-2(b). Here we presume a fixed blur disk of diameter d , across which we move disk D . If D were infinite (i.e. a straight edge) the intensity at the original in-focus edge would be exactly half the intensity of the uniform central region of the blurred image. As D decreases, the intensity at this point decreases. Also, as D decreases, the slope of the edge profile decreases near the outer edge and increases near the inner edge.

For a relatively small defocus, so that $d < D$, we see that the intensity at the center of the blurred image is independent of D . A cross-over occurs at $d = D$, corresponding to the plane containing "cross-over" point A in Fig. AI-1. For $d > D$, the intensity at the center of the blurred image decreases with D^2 , and the width of the blurred edge is essentially equal to the smaller value D . For example, for $D = d/2$, the circle moved across the blur disk in Fig. AI-2(b) has only half the diameter of the blur disk itself. Full amplitude is therefore reached half way across, as shown, and the amplitude is only $1/4$ as great (the common area being now only $1/4$ as great.)

The shape of the edge for $D = 2d$ and for $D = d/2$ is identical, except for scale, since in both cases we are simply convolving two circles of diametric ratio 2:1. For $D = d/2$, however, the height of the curve will be $1/4$ and the width $1/2$ that for $D = 2d$. In other words the slopes will be twice as great for the $D = 2d$ case. In general, the edge profiles will have identical form for $D = kd$ and $D = d/k$, though for $D = kd$, the central intensity will be k^2 times as high, the edge k times as wide, and the general slope k times as for $D = d/k$.

This general approach can be used to calculate the defocus image for any original in-focus pattern and any shape of blur disk, although the difficulty is of course greater the more complex the shape. For example, with a square lens aperture the blurred image would not have rotational symmetry.

Note that if the image in Fig. AI-1 were a long bar of width D , rather than a disk of diameter D , we would get different defocus profiles (since, in terms of Fig. AI-2, we would be convolving a circle and a straight edge, rather than two circles). However, we would get a cross-over point (i.e. point A in Fig. AI-1) in exactly the same plane.

APPENDIX II

LENS VIBRATION AS A MECHANISM FOR INCREASED DEPTH OF FIELD

An accommodation system can not only provide clear focus over a range of object distance, but can also provide the organism with an actual measure of distance in terms of the state of the control muscle or control signal. For example, experiments by Wallach and Norris (1963, p. 663) lead them to conclude that accommodation can function as a potent cue for distance. There are other techniques for improving clarity over an extended range, which, however, cannot give distance information. One example is simply a small pupil which gives a large depth of field. Walls (1963, page 254) notes a number of methods that have evolved for achieving increased depth of field. One of these involves the use of elongated receptors. He notes that

“... the visual elements of a squid are so enormously long that the image can recede and advance through their length, corresponding to great excursions of the object to and from the eye, without making any demands upon the inefficient apparatus of accommodation. Where vertebrates have very long visual cells, as in deep-sea fishes and some geckos, it is of course primarily for the sake of increasing their sensitivity, though as an incidental effect it partially obviates accommodation.”

Let us see how improved depth of field can be achieved with elongated receptors. Assume a receptor depth $2h$, as in Fig. AII-1, and to simplify the equations assume that each

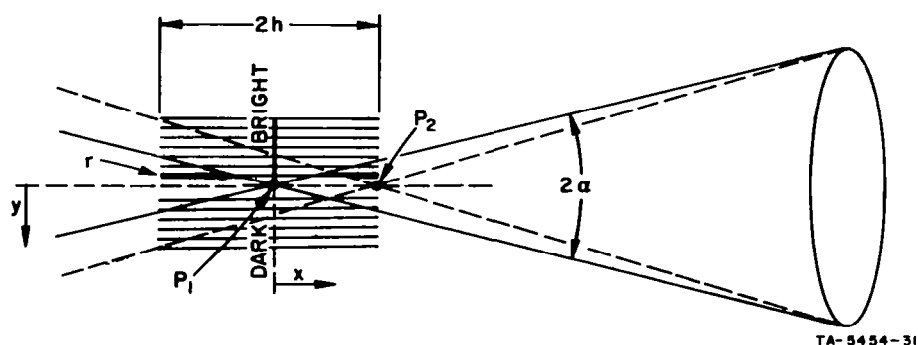


FIG. AII-1 GEOMETRY OF AN EDGE IMAGE FOCUSED WITHIN A STACK OF ELONGATED RECEPTORS

receptor responds simply to the total integrated light falling on it. For example, the total light received by receptor “ r ” in Fig. AII-1 is assumed to be proportional to the length of the two darkened regions. (In other words, we assume linear summation of the light and neglect the absorption of light as it passes through the receptor.)

Consider an edge brought to focus in the plane of point P_1 , so that the image is bright to the left of P_1 and dark to the right of P_1 . In any out-of-focus plane we assume a

linear edge transition with the intensity at the bright side the same as in the image plane; this is a good approximation for $2h$ small compared with the distance between the receptor stack and the lens. Under these conditions we can easily calculate the total light, $I(y)$, intercepted by each receptor as a function of its lateral position y . For $y > 0$ we can write

$$I(y) = 2 \int_{y/\tan \alpha}^h I_y(x) dx, \quad (\text{AII-1})$$

where 2α is the cone angle and $I_y(x)$ is the intensity variation along the receptor at lateral position y . The function $I_y(x)$ can be written

$$I_y(x) = k \left(\frac{x \tan \alpha - y}{2x \tan \alpha} \right), \quad (\text{AII-2})$$

where k is a constant, so that Eq. (AII-1) becomes

$$I(y) = k \left[x - \frac{y}{\tan \alpha} \ln x \right]_{y/\tan \alpha}^h \quad (\text{AII-3})$$

$$I(y) = k \left[\left(h - \frac{y}{\tan \alpha} \right) - \frac{y}{\tan \alpha} \ln \left(\frac{h \tan \alpha}{y} \right) \right].$$

Letting

$$\frac{y}{h \tan \alpha} = z, \quad (\text{AII-4})$$

Eq. (AII-3) becomes

$$I(y) = kh \left[(1-z) - z \ln \frac{1}{z} \right]. \quad (\text{AII-5})$$

Eq. (AII-5) has the form shown in Fig. AII-2 for $0 < z < 1$. It is simple to show that for negative values of z , i.e. to the left of P_1 , the curve has the same form but inverted. In other words, the edge profile has the form given by the curve of Fig. AII-2 where the width of the transition region depends on the value h according to Eq. (AII-4).

If the optical focus is now changed so that the in-focus edge falls at one end of the receptor stack, as suggested by point P_2 in Fig. AII-1, then Eq. (AII-1) is changed to

$$I(y) = \int_{y/\tan \alpha}^{2h} I_y(x) dx, \quad (\text{AII-1}')$$

and the resulting function is identical to that of Eq. (AII-5) except that

$$z = \frac{y}{2h \tan \alpha}; \quad (\text{AII-4}')$$

that is, the abscissa scale is doubled. Thus, shifting focus from the center of the stack to the end of the stack changes the profile curves from A to B , respectively, in Fig. AII-3. The corresponding edge profiles for a compressed stack (i.e. $h \approx 0$) fixed in the plane of P_1 would simply be a sharp edge A' and a linear transition edge B' , respectively.

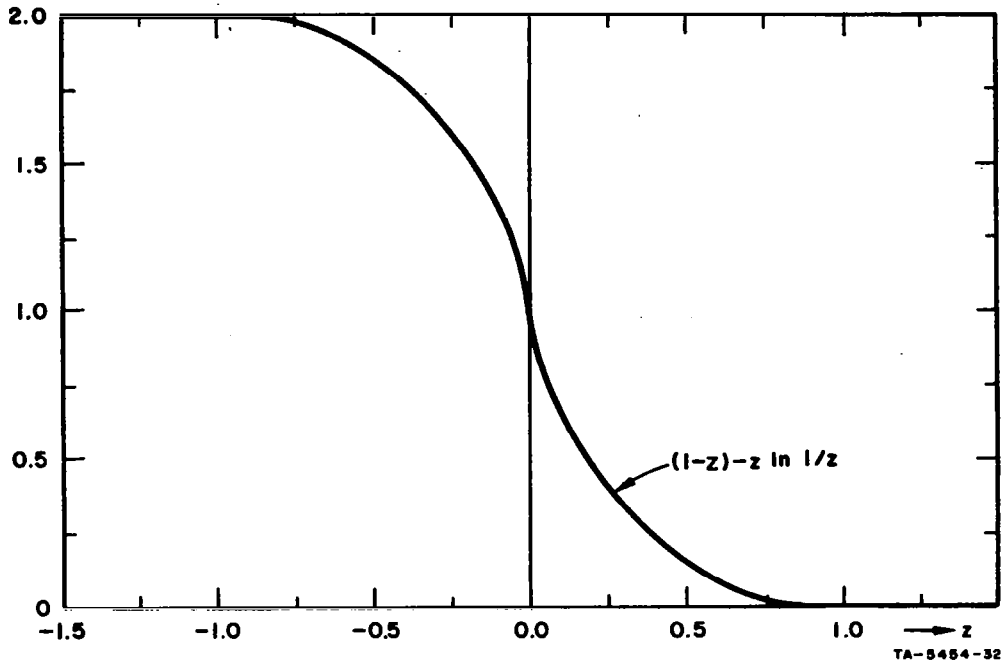


FIG. AII-2 EDGE PROFILE RESULTING FROM ARRANGEMENT IN FIG. AII-1

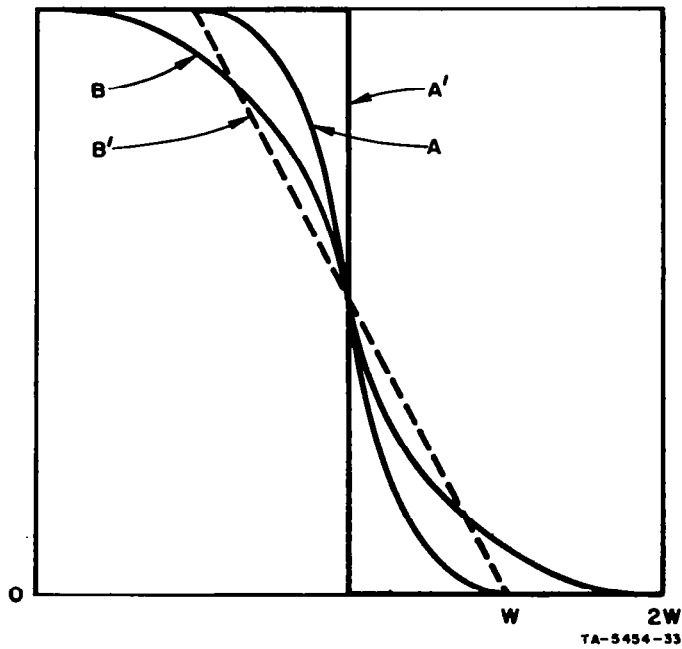


FIG. AII-3 EDGE PROFILES FOR DIFFERENT FOCUS POSITIONS WITHIN THE RECEPTOR STACK
 A—Profile when image plane is at center of stack
 B—Profile when image plane is at one surface of stack
 A' and B'—Corresponding profiles for thin stack

Thus, by elongating the receptor stack the sharp in-focus edge profile A' converts to smeared form A , whereas the linear transition curve B' (for a defocus corresponding to an image plane shift h) is sharpened to the form B . The edge width of curve B is twice that of curve B' , however, the slope is much greater at the center of the edge for curve B . In fact, the derivative at the center of the edge for curves A and B is infinite as can be seen by differentiating Eq. (AII-5) to obtain

$$\frac{dI(z)}{dz} = kh \ln z, \quad (\text{AII-6})$$

which is infinite at $z=0$, the center of the edge.

It can readily be seen that the edge curve for any other focus position on the stack will fall between the curves A and B . Any such curve will also have infinite slope at the edge center. For focus positions beyond either end of the stack however, the magnitude of derivative at the center of the edge decreases rapidly.

Thus, for focus positions within the depth of the stack the edge patterns have very sharp derivatives at the center regions of the edge. The ideally in-focus image is smeared to some extent (though the magnitude of derivative at the center of the edge is maintained), but the overall edge pattern of otherwise out-of-focus edges which fall within the stack is much improved, at least in the center region of the edge profile. We seem then to have the potential for improved depth of focus, though with some deterioration of the best focus.

The results obtained with an elongated stack are duplicated with a thin stack which is made to vibrate back and forth over the same range $2h$, or with a fixed retina and a refractive vibration that swings the in-focus image over the same range. In the latter two cases we have to assume that the net effect depends on the average intercepted light over a cycle of vibration.

Recall that Arnulf and Dupuy, Fig. III-2, found that the amplitude of accommodation fluctuations increased tenfold when accommodation increased from infinity to 6.8 diopters, or about 15 cm. This increase in amplitude was relatively smooth and monotonic from one extreme to the other, with the vibration amplitude finally reaching not simply a "few tenths diopter" but as much as 1 to 2 diopters.

A steady defocus of 2 diopters is very large, well beyond the depth of field. Certainly a much smaller amplitude would be adequate for any purpose of focus control. We began to wonder whether these large vibrations might have another function, namely an increase in effective depth of field in the manner discussed here. For strong accommodation (i.e. close-up) the depth of field is very small in terms of physical distance and an increased depth of field would certainly be a reasonable function to strive for. A primary question is whether a 2 cps vibration is rapid enough to effectively achieve the integration discussed above.

In Sec. IX we speculated that these vibrations were not vibrations in the usual sense, but simply normal accommodation corrections (what we called "accommodation saccads"). But simply assigning a different "cause" to the vibration does not affect whether the vibration has in fact any effect on depth of field. We might note that with our new hypothesis we should expect the vibration amplitude to be large whenever the accommodation error is likely to be high (so that each correction movement will be relatively large), and under these conditions we could argue a need for increase in effective depth of field.

It is not clear at this time whether these vibrations actually have any effect on depth of field, although the possibility exists. In this connection we might note some comments in a paper by "W. MACD" (1942), in which are described experiments on sweeping the image plane while exposing a photographic film. A significant increase in depth of field is reported, but with a focus that is considered "slightly softer throughout the entire range." In the configuration of "W. MACD's" experiment, the field was swept by axially vibrating one lens of a compound lens system. The optics were specially arranged so that blurring occurred with minimal lateral shift of the picture parts. They noted that:

"Experimental results proved promising as objects in each plane within a scene appeared to the eye to be in sharp focus despite superimposing of sharp images over 'fuzzy' images. The individual photographic impressions within a single exposure were in good 'register' insofar as size was concerned and a good resistivity apparently permitted sharp impressions to 'mask' fuzzy impressions to a satisfactory extent."

One basis on which to decide what sort of vibration amplitude might be reasonable for purposes of improved depth of field is to consider the degree of general focus deterioration with this vibration (the "soft" focus effect noted by "W. MACD"). We have seen that an ideally focused edge would be smeared according to the curve A in Fig. AII-3; the larger the magnitude of vibration the larger the width of the smear. For a ± 1 diopter variation, the total width $2W$ would be about $10'$ of arc; that is, $(1/60) 3 \text{ mm} = 50\mu \approx 10'$, assuming a total average refraction of 60 diopters. But the neural unit of Fig. VI-2 was seen to have just about this radial extent, so that we could expect considerable sharpening of an edge smeared out over $10'$ of arc or so. Thus, the smear obtained with a normal sized pupil and a ± 1 diopter refractive vibration is in the range in which we might get significant sharpening from neural-unit processing.

But this is all speculation. This discussion is meant to be merely suggestive since there is as yet no evidence that these vibrations play any role in depth of field. It is simply interesting that the possibility exists and that certain relevant numbers are at least of the right order of magnitude.